The stem cell transcription factor ZFP57 induces IGF2 expression to promote anchorage-independent growth in cancer cells.

Yuhki Tada[1], Yukari Yamaguchi[2], Tomoaki Kinjo[1], Xiahong Song[1], Tadayuki Akagi[1], Hiroyuki Takamura[2], Tetsuo Ohta[2], Takashi Yokota[1] and Hiroshi Koide[1]

[1]Department of Stem Cell Biology, Graduate School of Medical Sciences, Kanazawa University, Ishikawa, Japan, and [2]Department of Gastroenterologic Surgery, Graduate School of Medical Sciences, Kanazawa University, Ishikawa, Japan.

Correspondence: Hiroshi Koide, Department of Stem Cell Biology, Graduate School of Medical Sciences, Kanazawa University, 13-1, Takara-machi, Kanazawa, Ishikawa 920-8640, Japan. Tel: +76-265-2207. Fax: +76-234-4238. E-mail: hkoide@med.kanazawa-u.ac.jp

Keywords: ZFP57, IGF2, anchorage-independent growth, HT1080, transformation, oncogene

Running title: ZFP57 promotes anchorage-independent growth.

Abstract

Several common biological properties between cancer cells and embryonic stem (ES) cells suggest the possibility that some genes expressed in ES cells might play important roles in cancer cell growth. The transcription factor ZFP57 is expressed in self-renewing ES cells and its expression level decreases during ES cell differentiation. This study showed that ZFP57 is involved in the anchorage-independent growth of human fibrosarcoma HT1080 cells in soft agar. ZFP57 overexpression enhanced, while knockdown suppressed, HT1080 tumor formation in nude mice. Furthermore, ZFP57 regulates the expression of IGF2, which plays a critical role in ZFP57-induced anchorage-independent growth. ZFP57 also promotes anchorage-independent growth in ES cells and immortal fibroblasts. Finally, immunohistochemical analysis revealed that ZFP57 is overexpressed in human cancer clinical specimens. Taken together, these results suggest that the ES-specific transcription factor ZFP57 is a novel oncogene.

Introduction

Embryonic stem (ES) cells are derived from pluripotent cells of the early mammalian embryo and are capable of unlimited, undifferentiated proliferation *in vitro*.[1,2] Leukemia inhibitory factor (LIF) can maintain the self-renewal and pluripotency of mouse ES cells.[3] Similarly, several transcription factors play important roles in the self-renewal of ES cells.[4] For example, the POU-family transcription factor Oct3/4 is an essential player in self-renewal and often acts together with the SRY-related HMG-box protein Sox2 to regulate the expression of transcription factors important to self-renewal.[5-7] Nanog is a homeobox transcription factor whose overexpression can bypass the requirement for LIF in self-renewal, although it is dispensable for self-renewal.[8-10] Extensive studies have revealed that these transcription factors form networks and stimulate the expression of a set of genes that maintain self-renewal in ES cells.[11,12]

Interestingly, ES cells share many biological properties with cancer cells. For example, when injected into nude mice, ES and cancer cells can produce benign and malignant tumors, respectively. Both cell types have a rapid cell cycle. Telomerase activity is very high in both cells, which allows them to proliferate indefinitely. In

addition, several signal transduction pathways seem to be commonly used in both ES cell self-renewal and cancer cell growth.[13,14] For example, the STAT3 pathway, which plays a central role in ES cell self-renewal,[15,16] is activated in several types of cancer cells.[17] The Wnt/β-catenin pathway, whose activation is associated with tumorigenesis in many tissues,[18] is involved in ES cell self-renewal.[19-21] Gli, a central signaling molecule in the Hedgehog pathway that is activated in a broad spectrum of human tumors,[22] promotes the maintenance of ES cells.[23] These similarities have raised the possibility that some molecules involved in ES cell self-renewal may play important roles in cancer cell growth and encouraged us to search for an oncogene in self-renewing ES cells.

Here, we report the involvement of the ES-specific transcription factor ZFP57 in cancer cell growth. We demonstrate that ZFP57 is involved in the anchorage-independent growth of human fibrosarcoma HT1080 cells both *in vitro* and *in vivo* and that it acts by regulating the expression of insulin-like growth factor 2 (IGF2). In addition, we show that this transcription factor is also involved in the growth of mouse ES cells in soft agar and can stimulate the anchorage-independent growth of mouse NIH3T3 cells. Furthermore, we observed the overexpression of ZFP57 in tumor tissues from cancer patients, suggesting that ZFP57 is a novel

oncogene.

Results

Search for stem cell genes that promote anchorage-independent growth in HT1080 cells

To identify stem cell genes involved in tumor growth, we cloned several genes from self-renewing mouse ES cells and examined the effect of their ectopic expression on anchorage-independent growth, a property of cancer cells important for tumor formation (Supplementary Figure S1). As a result, we found that Lrh1 (also known as Nr5a2), Nanog and Zfp57 can promote anchorage-independent growth in human fibrosarcoma HT1080 cells. The involvement of LRH1 and NANOG in tumor growth has already been reported.[24,25] In this study, therefore, we focused our attention on ZFP57.

Involvement of ZFP57 in the anchorage-independent growth of HT1080 cells

Since we used mouse Zfp57 for screening, we first confirmed that human ZFP57 also promotes anchorage-independent growth. As shown in Figures 1a-c, overexpression of human ZFP57 enhanced the growth of HT1080 cells in soft agar. We next examined the requirement of ZFP57 for anchorage-independent growth in HT1080 cells

by knockdown experiments using artificial micro RNA (miRNA) against ZFP57. To avoid any off-target effect, we used two independent ZFP57 miRNA constructs, ZFP57 miRNA(349) and ZFP57 miRNA(427). Quantitative RT-PCR confirmed that both ZFP57 miRNAs suppress the expression of endogenous ZFP57 mRNA (Figure 3b). Using these miRNAs, we found that ZFP57 knockdown suppresses the growth of HT1080 in soft agar (Figure 1d). We confirmed that the suppression of soft agar growth by ZFP57 miRNA can be restored by overexpression of Zfp57 (Supplementary Figure S2). These results suggest that ZFP57 is involved in the anchorage-independent growth of HT1080 cells.

ZFP57 is involved in tumor formation in nude mice

To determine whether ZFP57 is required for anchorage-independent growth in HT1080 cells *in vivo*, we established a HT1080 transfectant in which ZFP57 can be knocked down by the addition of 4-hydroxytamoxifen (4-HT) (Supplementary Figure S3). We confirmed that 4-HT treatment reduces the expression of ZFP57 and suppresses growth in soft agar. After pretreatment with 4-HT, we implanted the transfectant cells into nude mice subcutaneously and measured the size of HT1080-derived tumors. We observed that the depletion of ZFP57 suppresses tumor growth in nude mice (Figure 2a).

We next examined the effect of ZFP57 overexpression on HT1080 tumor formation. As in the case of *in vitro* experiments, we observed that the overexpression of ZFP57 promotes tumor growth *in vivo* (Figure 2b). Overexpression of ZFP57 in the resulting tumors was confirmed by quantitative RT-PCR (Supplementary Figure S4). These results indicate that ZFP57 is involved in anchorage-independent growth in HT1080 cells both *in vitro* and *in vivo*.

IGF2 is a downstream gene of ZFP57

To elucidate the molecular mechanism behind ZFP57-mediated anchorage-independent growth, we searched for a target gene of ZFP57. In embryo and ES cells, Zfp57 regulates the expression of a variety of imprinted genes.[26,27] Among imprinted genes, IGF2 is involved in tumorigenesis in various cancers.[28,29] We therefore explored the possibility that IGF2 may be a downstream gene of ZFP57 in HT1080 cells.

Based on previous reports showing binding of ZFP57 to the imprinting control region (ICR) of IGF2-H19 in ES cells,[27] we first examined whether the same was true in HT1080 cells. ChIP analysis revealed that ZFP57 binds to the region containing the ZFP57-binding motif within the IGF2-H19 ICR in HT1080 cells (Figure 3a). Furthermore, we found that IGF2 expression is suppressed upon knockdown of ZFP57

(Figure 3b). We confirmed that the ZFP57 knockdown-mediated suppression of IGF2 expression can be recovered by Zfp57 overexpression (Supplementary Figure S5). These results suggest that ZFP57 regulates IGF2 expression in HT1080 cells.

IGF2 is required for anchorage-independent growth in HT1080 cells

Since we identified IGF2 as a downstream gene of ZFP57, we explored the possibility that IGF2 may be required for the ZFP57-mediated anchorage-independent growth of HT1080 cells.

Firstly, we assessed the existence of functional IGF2 signaling in HT1080 cells. To induce cell proliferation and survival, IGF2 must bind to the IGF1 receptor and thereby activate AKT.[28,29] Western blot analysis revealed that the IGF1 receptor is expressed in HT1080 cells (Figure 4a). When we stimulated HT1080 cells with recombinant human IGF2 in serum-free conditions, we observed AKT phosphorylation at Thr-308 and Ser-473, indicating activation of AKT (Figure 4b). These observations suggest that the IGF2 signaling pathway is functional in HT1080 cells.

Next, we examined the effect of ZFP57 knockdown on the phosphorylation status of AKT. When we compared the amount of phosphorylated AKT between ZFP57 knockdown HT1080 cells and control HT1080 cells, we found that ZFP57

knockdown reduces AKT phosphorylation (Figure 4c), suggesting that ZFP57-stimulated IGF2 upregulation leads to AKT activation in HT1080 cells.

To examine the requirement of IGF2 in anchorage-independent growth in HT1080 cells, we inhibited IGF2 activity with an anti-IGF2 neutralizing antibody. As shown in Figure 4d, the neutralizing antibody strongly suppressed anchorage-independent growth. Similar results were obtained with knockdown experiments (Figure S6). Furthermore, the neutralizing antibody suppressed the ZFP57-induced anchorage-independent growth of HT1080 cells (Figure 4e).

We also examined the requirement of IGF2 in tumor formation by xenograft assay (Figure 4f). When IGF2 knockdown HT1080 cells were implanted into nude mice, IGF2 knockdown significantly inhibited tumor formation. Moreover, we found that IGF2 knockdown attenuates the enhanced tumor growth by Zfp57 overexpression (Figure 4g and supplementary Figure S7).

These results suggest that IGF2 is a key molecule in ZFP57-mediated anchorage-independent growth.

Zfp57 is involved in the anchorage-independent growth of ES cells

ES cells can grow in anchorage-independent conditions, as expected from the fact that

they can give rise to benign tumors called teratomas when injected into immunodeficient mice.[3] Previously, we established Zfp57 knockout ES cells and showed that Zfp57 is dispensable for ES cell self-renewal and proliferation in anchorage-dependent conditions.[30] Since we found here that ZFP57 is involved in anchorage-independent growth in HT1080 cells, we examined whether this was true in ES cells. To assess the effect of Zfp57 level on the colony-forming capacity of ES cells in soft agar, we compared 1F9 cells (*Zfp57*$^{+/-}$ ES cells that express Zfp57) to 2E9 cells (*Zfp57*$^{-/-}$ ES cells that lost expression of Zfp57).[30] Both cells were seeded into soft agar and allowed to grow. About 1 week later, we observed that the number of viable 2E9 colonies was significantly lower than that of viable 1F9 colonies (Figure 5), suggesting that Zfp57 is involved in anchorage-independent growth in ES cells. We confirmed that the reduction in colony number can be recovered by overexpression of exogeneous Zfp57 (Supplementary Figure S8). These results further suggest that ZFP57 plays an important role in anchorage-independent growth.

ZFP57 transforms NIH3T3 cells

The importance of ZFP57 in anchorage-independent growth encouraged us to explore the possibility that ZFP57 may be an oncogene. The immortal mouse fibroblast cell

line NIH3T3 can hardly grow in an anchorage-independent manner and has been used to evaluate the transforming activity of individual genes.

To determine whether ZFP57 has transforming potential, we overexpressed ZFP57 in NIH3T3 cells and performed a soft agar assay. As shown in Figure 6, colony formation in soft agar by parental NIH3T3 cells was very ineffective. By contrast, ZFP57 overexpression allowed NIH3T3 cells to grow efficiently in soft agar, suggesting that ZFP57 possesses oncogenic properties.

ZFP57 expression in cancer patients

Finally, we investigated the expression of ZFP57 in patients with different kinds of cancers by immunohistochemical staining. When compared to normal tissues, we observed the overexpression of ZFP57 in several cancer tissues (Figure 7, Table I). In pancreatic cancer, more than 70% of the patients tested were positive for ZFP57. In gastric, breast, colon and esophageal cancer tissues, about 40% of the patients were ZFP57-positive. By contrast, ZFP57 overexpression was rarely observed in hepatocellular carcinoma and cholangiocellular carcinoma tissues. The specificity of anti-human ZFP57 antibody was confirmed by Western blotting (Supplementary Figure S9). These results suggest that ZFP57 functions as an oncogene in some human

cancers.

Moreover, we performed immunohistochemical staining using anti-IGF2 antibody (Supplementary Figure S10) and found a statistically significant correlation between ZFP57 and IGF2 expression in esophageal and breast cancers (P=0.03169 and 0.00617, respectively, Chi-square test). No significant correlation was observed in other cancers. These results suggest that ZFP57 overexpression leads to IGF-2 overexpression in some types of cancers.

Discussion

The transcription factor Zfp57 was originally identified as an undifferentiated cell-specific gene in F9 embryonal carcinoma cells.[31] The mouse ZFP57 protein consists of 421 amino acids and contains one Kruppel-associated box (KRAB) domain and five zinc fingers, while the human ZFP57 protein consists of 536 amino acids with one KRAB domain and seven zinc fingers. In ES cells, Zfp57 is downstream of Stat3 and Oct3/4, and therefore shows self-renewal-specific expression.[30] In adult mouse organs, Zfp57 is highly expressed in testis and brain.[31,32] Loss of the zygotic function

of Zfp57 causes partial lethality, while eliminating both the maternal and zygotic functions of Zfp57 leads to complete embryonic lethality.[26] Several reports have suggested that this transcription factor binds to KRAB-associated protein 1 (KAP1), a scaffold protein for various heterochromatin-inducing factors, through its KRAB domain, and is involved in genome imprinting by recruiting KAP1 to several ICRs.[26,27,33] In addition, mutations in the *ZFP57* gene result in transient neonatal diabetes mellitus type 1, possibly through Plagl1 overexpression.[34,35] The role of ZFP57 in tumorigenesis has not been elucidated yet.

In this study, we demonstrated the involvement of ZFP57 in the anchorage-independent growth of tumor cells both *in vitro* and *in vivo*. When cultured in the absence of adhesion to substratum, normal adherent cells undergo apoptosis, a phenomenon known as anoikis.[36,37] By contrast, transformed cells are able to survive and grow even in the absence of anchorage. Anchorage-independent growth is therefore a major characteristic of transformed cells, and in fact shows a good correlation with tumor malignancy.[38,39] In addition to cancer cells, Zfp57 is involved in ES cell anchorage-independent growth, suggesting that ZFP57-mediated anchorage-independent growth is not restricted to cancer cells. Furthermore, ZFP57 enables immortal NIH3T3 fibroblasts to proliferate independently of anchorage.

These results strongly suggest that ZFP57 plays an important role in anchorage-independent growth.

We demonstrated that, as a molecule downstream of ZFP57, IGF2 plays a critical role in anchorage-independent growth in HT1080 cells. To promote cell proliferation, IGF2 binds to the IGF1 receptor and stimulates PI3 kinase activity, leading to the activation of AKT. It is well-known that AKT activation plays an important role in anchorage-independent growth in cancer cells.[37] We confirmed the expression of the IGF1 receptor and observed that IGF2 stimulation leads to activation of AKT in HT1080 cells. Furthermore, we found that ZFP57 knockdown reduces AKT phosphorylation. These observations suggest that ZFP57-induced IGF2 stimulates HT1080 cells in an autocrine manner and activates the AKT pathway to avoid anoikis and promote anchorage-independent growth.

Although overexpression of IGF2 is observed in a variety of cancer cells,[40] its molecular mechanism is not fully understood. A well-known mechanism is loss of imprinting. In normal cells, IGF2 expression is regulated by genome imprinting and transcription of IGF2 mRNA occurs only at the paternal allele. In some cancer cells, however, this imprinting system is not functional and IGF2 mRNA is transcribed from both alleles, resulting in increased expression of IGF2. Imprinting of IGF2 is

regulated at the IGF2-H19 ICR, and ZFP57 binds to this region in ES cells.[27] In this study, we also observed the binding of ZFP57 to the IGF2-H19 ICR in HT1080 cells. It is possible therefore that ZFP57 regulates IGF2 expression through loss of imprinting in HT1080 cells, although the previous finding that Zfp57 deficiency has no effect on the expression level of Igf2 in mouse embryo cells does not support this possibility.[26] Our preliminary analysis using bisulfite sequencing suggests that DNA methylation level around the ZFP57-binding region of IGF2-H19 ICR is low in HT1080 cells, also diminishing this possibility. Another mechanism of IGF2 overexpression is through activation of the IGF2 promoter. For example, E2F3 activates the IGF2 promoter and overexpression of E2F3 correlates with IGF2 overexpression in prostate and bladder cancers,[41] suggesting that IGF2 expression in cancer cells is modulated not only by imprinting, but also by regulation of IGF2 promoter activity. We are now investigating which mechanism of IGF2 upregulation is employed by ZFP57.

Since ZFP57 regulates the expression of various imprinted genes and since the aberrant regulation of imprinted genes causes tumorigenesis,[42,43] it is possible that other imprinted genes, in addition to IGF2, may function downstream of ZFP57 to promote tumorigenesis. Interestingly, we have already found that ZFP57 regulates the expression of Delta-like homolog 1 (DLK1) in HT1080 cells (Tada *et al.*, unpublished

data). An imprinted gene, *DLK1*, is a non-canonical Notch ligand that plays an important role in the growth of several tumors including neuroblastoma and hepatoblastoma.[44] It is possible therefore that *DLK1* may be another key imprinted gene in ZFP57-stimulated cancer growth. In addition, non-coding RNAs are possible target genes of ZFP57, since multiple non-coding RNAs are located in the imprinted locus and are involved in tumorigenesis.[45-47] Identification of another ZFP57 target gene would be of great help to understand the molecular mechanism of ZFP57-induced tumor growth in more detail.

In conclusion, we demonstrated here that the ES-specific transcription factor ZFP57 promotes anchorage-independent growth in HT1080 cells by upregulating IGF2 expression. In addition, ZFP57 enables normal mouse fibroblasts to grow even in the absence of anchorage. Furthermore, we observed the overexpression of ZFP57 in multiple types of cancers. Our data suggest that ZFP57 can function as an oncogene. Our present findings raise several intriguing possibilities. Firstly, since ZFP57 is overexpressed in several tumors, together with the previous findings that ZFP57 is involved in imprinting, it is possible that aberrant regulation of ZFP57 may cause loss of imprinting in some types of cancers. Secondly, considering that ZFP57 is a stem cell-specific transcription factor involved in tumor growth, it is possible that ZFP57

may be expressed in cancer stem cells and play a role in their growth. Thirdly, since induced pluripotent stem (iPS) cells have a similar gene expression profile to ES cells,[48] it is likely that ZFP57 is expressed in iPS cells. Considering that ZFP57 has transforming ability, it is possible that the high expression of ZFP57 in iPS cells may increase the risk of tumor formation during cell therapy using iPS-derived cells. These possibilities will be explored in a future study.

Materials and methods

Cell lines and antibodies

HT1080 fibrosarcoma cells and HEK293 cells were cultured in Dulbecco's modified Eagle's medium (DMEM) (Nacalai Tesque, Kyoto, Japan) supplemented with 10% fetal bovine serum. NIH3T3 cells were cultured in DMEM containing 10% fetal calf serum. ES cells were cultured on gelatin-coated dishes with LIF-supplemented DMEM as described previously,[49] except that the culture medium contained 150 μM 1-thioglycerol (Wako Pure Chemical Industries, Osaka, Japan) instead of 40 μM β-mercaptoethanol. All cell lines were maintained in a humidified atmosphere of 5% CO_2.

Anti-IGF2 neutralizing antibody (clone S1F2) was purchased from Millipore (Billerica, MA, USA). Control IgG (ab37355) was from Abcam (Cambridge, MA, USA). Anti-myc antibody (clone 9E10) and anti-α-tubulin antibody (clone 2F9) were from Santa Cruz Biotechnology (Santa Cruz, CA, USA) and MBL (Nagoya, Japan), respectively. Antibodies against AKT (#4691), phospho-AKT (Thr308) (#2965), phospho-AKT (Ser473) (#4060) and the IGF1 receptor (#9750) were from Cell Signaling Technology (Boston, MA, USA).

Plasmid construction

The coding sequences of human and mouse ZFP57 (NCBI accession numbers: NM_001109809 and NM_009559, respectively) were amplified from cDNA synthesized from HT1080 cell total RNA and A3-1 ES cell total RNA, respectively, using primers listed in Supplementary Table S1. pCAGIP-myc-hZFP57, pCAGIP-HA-hZFP57 and pCAGIP-Flag-hZFP57 were constructed by inserting a myc-, HA- or flag-tagged human ZFP57 coding fragment into the mammalian expression vector pCAG-IP.[49] Plasmid pCAG-IH3 was constructed by replacing the sequence of internal ribosomal entry site (IRES) and the puromycin-resistance gene of pCAG-IP with that of IRES and the hygromycin-resistance gene of pIRES-hyg3 (Clontech, Palo

Alto, CA, USA). Plasmid pCAG-IN3 was constructed by inserting the CAG promoter of pCAG-IP into pIRES-neo2 (Clontech). Plasmids pCAGIH3-mZfp57 and pCAGIN3-myc-mZfp57 were produced by inserting a mouse Zfp57 coding fragment and a myc-tagged mouse Zfp57 coding fragment into pCAG-IH3 and pCAG-IN3, respectively. To construct the episomal expression vector pEBM-CAGIP, EBNA1 cDNA and the OriP sequence of Epstein-Barr virus were transferred from pEBMulti-Neo (Wako Pure Chemical Industries) to pCAG-IP. The coding region of the ligand-binding domain of the estrogen receptor was inserted into pCAGPMN(PvuII-MfeI)-CreER, a kind gift from Dr. Chuanhai Sun, to produce pCAG-myc-ER-Cre-ER.

For knockdown experiments by RNA interference, oligonucleotides containing target sequences for ZFP57 [5'-GGTCCTTTACCAGGATGTTAT-3' for ZFP57(349); 5'-GCTAATCACCAAGCTTGAGCA-3' for ZFP57(427)] and IGF2 [5'-GCTGGTGCTTCTCACCTTCTT-3' for IGF2(779)] were introduced into the miRNA expression vector pcDNA6.2-GW/EmGFPmiR (Invitrogen, Carlsbad, CA, USA) to obtain pGW/EmGFP-ZFP57(349 or 427) and pGW/EmGFP-IGF2(779), respectively (Supplementary Table S1). EmGFP-control miRNA, EmGFP-ZFP57 miRNA(349 or 427) and EmGFP-IGF2 miRNA(779) were transferred from

pGW/EmGFP constructs to pEBM-CAGIP to obtain pEBM-CAGIP-EmGFP-control, pEBM-CAGIP-EmGFP-ZFP57(349 or 427) and pEBM-CAGIP-EmGFP-IGF2(779), respectively. The plasmid pCAG-IG1a was constructed by replacing the IRES-puromycin resistance gene of pCAG-IP with IRES-hrGFP1a in pIRES-hrGF1a (Stratagene, La Jolla, CA, USA). An inducible expression vector, pCALiPL-IG1a, was constructed by inserting a loxP-IRES-puromycin resistance-loxP cassette into pCAG-IG1a. EmGFP-ZFP57 miRNA(427) was transferred from pGW/EmGFP-ZFP57(427) into pCALiPL-IG1a to produce pCALiPL-IG1a-EmGFP-hZFP57(427).

Establishment of stable cell lines

To establish ZFP57-overexpressing HT1080 cells, HT1080 cells were transfected with pCAGIP-myc-hZFP57 using Lipofectamine 2000 (Invitrogen) and selected with 0.3 μg/ml puromycin for 2 weeks. Resistant clones were pooled and subjected to experiments. Similarly, HT1080 cells were transfected with pEBM-CAGIP-EmGFP constructs to obtain HT1080 cells with ZFP57 knockdown.

To establish the cell line with inducible ZFP57 knockdown HT1080/pCALiPL-ZFP57(427), HT1080 cells were transfected with both

pCALiPL-IG1a-EmGFP-hZFP57(427) and pCAG-myc-ER-Cre-ER, and selected with puromycin. Each resistant clone was assessed for 4-HT-dependent knockdown of ZFP57.

Quantitative RT-PCR

Total RNA was extracted from individual cultured cells using Sepasol RNA I super G (Nacalai Tesque), and cDNA synthesis was performed with ReverTra Ace (Toyobo, Osaka, Japan). Real-time PCR analysis using SYBR green was conducted using the Mx3000p System (Stratagene), and results were normalized to β-actin expression. Primers are listed in Supplementary Table S1.

Western blot analysis

Cells were lysed in cell lysis buffer [20 mM Hepes-NaOH (pH 7.2), 10 mM $MgCl_2$, 1 mM EDTA, 10 mM sodium fluoride, 25 mM β-glycerophosphate, 1 mM sodium orthovanadate, 20 μg/ml aprotinin, 10 μg/ml leupeptin, 10 μg/ml pepstatin A, 1% Nonidet P-40, and 10% glycerol]. Lysates were then mixed with 1X sample buffer [6% glycerol, 10 mM Tris–HCl (pH 6.8), 2% SDS, 50 mM DTT, 2 mM EDTA, and 0.002% Coomassie Brilliant Blue R250] and heat-denatured. Samples were subjected

to SDS-PAGE and electrophoretically transferred to nitrocellulose membranes. The membranes were then probed with antibodies, and signals were visualized using enhanced chemiluminescence reagents (Perkin-Elmer, Norwalk, CT, USA) with the LAS-1000 image analyzer (Fuji Film, Tokyo, Japan). In all experiments, α-tubulin was used as an internal control.

Soft agar assay and xenograft experiments

For soft agar assays, cells were seeded in 2.4 ml of culture medium containing 0.5% Sea Plaque agarose (Lonza, Rockland, ME, USA), overlaid on 3 ml of 0.53% agarose in 6 cm dishes. The cultures were maintained for about 2 weeks. Viable colonies were stained with 3-(4,5-di-methylthiazol-2-yl)-2,5-diphenyltetrazolium bromide (MTT) (Nacalai Tesque). Dishes were then scanned with an ES-2200 scanner (EPSON, Nagano, Japan), and the number of stained colonies was counted by Image-J (NIH, Bethesda, MD, USA).

The tumorigenic potential of HT1080/pCALiPL-ZFP57 cells was assessed in 10 CAnN,Cg-*Foxn1*^{nu}/CrlCrlj mice at 3 weeks of age (Charles River, Wilmington, MA, USA). After a 3 day treatment with ethanol or 4-HT, HT1080/pCALiPL-ZFP57 cells (1×10^7 cells/ml) were resuspended in the culture medium, and one million cells were

injected subcutaneously into mice. Animals were sacrificed 2 weeks after injection. Tumors were dissected and photographed. All procedures were conducted in accordance with the Fundamental Guidelines for Proper Conduct of Animal Experiment and Related Activities in Academic Research Institutions under the jurisdiction of the Ministry of Education, Culture, Sports, Science and Technology of Japan and approved by the Committee on Animal Experimentation of Kanazawa University.

Chromatin immunoprecipitation (ChIP) assay

HT1080 cells were transfected with pCAGIP-Flag-hZFP57 and cultured for 2 days. After harvest, cells were processed for ChIP assay using the OneDay ChIP kit (Nippon Gene, Tokyo, Japan). Briefly, cells were fixed with 1% formaldehyde for 10 min at room temperature and the chromatin was sheared to an average fragment size of 500–1000 bp by sonication with a Bioruptor (Cosmo Bio, Tokyo, Japan). After cross-linking was quenched with glycine, whole cell extracts were prepared for chromatin immunoprecipitation. Fragmented chromatin was used in each reaction. DNA was immunoprecipitated with 5 μg of anti-flag antibody (M2; Sigma) or normal mouse IgG (sc-2025; Santa Cruz). DNA from the immunoprecipitates or from 1% of the input material was analyzed by PCR using primers specific for the IGF2-H19 ICR

(Supplementary Table S1).

Immunohistochemical analysis

The expressions of ZFP57 and IGF2 in carcinomas were examined immunohistochemically using the EnVision+ System (DAKO, Copenhagen, Denmark). Tumor specimens were fixed in 10% formalin and embedded in paraffin. Dewaxed 4 μm sections were incubated with protein-blocking serum for 10 min to block non-specific binding. The sections were then incubated with rabbit anti-human ZFP57 polyclonal antibody (U-18; Santa Cruz Biotechnology) (1:50) or rabbit anti-human IGF2 polyclonal antibody (LS-B7415; LifeSpan Biosciences, Seattle, WA, USA) (5 μg/ml) at 4˚C overnight. After washing, EnVision+ polymer solution was applied for 1 hour. The reaction products were visualized with diaminobenzidine. The specimens were then lightly counterstained with hematoxylin. Written consent was obtained from all patients, and the project was approved by the Ethics Committee for Human Genome/Gene Analysis Research at Kanazawa University Graduate School of Medical Sciences.

Conflict of interest

The authors declare no conflict of interest.

Acknowledgments

We are grateful to Drs. Chuanhai Sun and Hitoshi Niwa for providing pCAGPMN(PvuII-MfeI)-CreER and pBRPyCAG-fKlf4-DsRed-IP, respectively. We also thank the Center for Biomedical Research and Education at Kanazawa University for the use of their DNA sequencer. This work was partly supported by Grants-in-Aid for Scientific Research from the Ministry of Education, Culture, Sports, Science and Technology of Japan, a grant from the Hokkoku Foundation for Cancer Research, and an Extramural Collaborative Research Grant from the Cancer Research Institute, Kanazawa University.

Supplementary Information accompanies the paper on the Oncogene website (http://www.nature.com/onc).

References

1 Evans MJ, Kaufman MH. Establishment in culture of pluripotential cells from mouse embryos. *Nature* 1981; **292**: 154-156.

2 Martin GR. Isolation of a pluripotent cell line from early mouse embryos cultured in medium conditioned by teratocarcinoma stem cells. *Proc Natl Acad Sci USA* 1981; **78**: 7634-7638.

3 Smith AG. Embryo-derived stem cells: Of mice and men. *Annu Rev Cell Dev Biol* 2001; **17**: 435-462.

4 Niwa H. How is pluripotency determined and maintained? *Development* 2007; **134**: 635-646.

5 Nichols J, Zevnik B, Anastassiadis K, Niwa H, Klewe-Nebenius D, Chambers I *et al*. Formation of pluripotent stem cells in the mammalian embryo depends on the POU transcription factor Oct4. *Cell* 1998; **95**: 379-391.

6 Niwa H, Miyazaki J, Smith AG. Quantitative expression of Oct-3/4 defines differentiation, dedifferentiation or self-renewal of ES cells. *Nat Genet* 2000; **24**: 372-376.

7 Masui S, Nakatake Y, Toyooka Y, Shimosato D, Yagi R, Takahashi K *et al*. Pluripotency governed by Sox2 via regulation of Oct3/4 expression in mouse

embryonic stem cells. *Nat Cell Biol* 2007; **9**: 625-635.

8 Chambers I, Colby D, Robertson M, Nichols J, Lee S, Tweedie S *et al*. Functional expression cloning of Nanog, a pluripotency sustaining factor in embryonic stem cells. *Cell* 2003; **113**: 643-655.

9 Mitsui K, Tokuzawa Y, Itoh H, Segawa K, Murakami M, Takahashi K *et al*. The homeoprotein Nanog is required for maintenance of pluripotency in mouse epiblast and ES cells. *Cell* 2003; **113**: 631-642.

10 Chambers I, Silva J, Colby D, Nichols J, Nijmeijer B, Robertson M *et al*. Nanog safeguards pluripotency and mediates germline development. *Nature* 2007; **450**: 1230-1234.

11 Boyer LA, Lee TI, Cole MF, Johnstone SE, Levine SS, Zucker JP *et al*. Core transcriptional regulatory circuitry in human embryonic stem cells. *Cell* 2005; **122**: 947-956.

12 Loh YH, Wu Q, Chew JL, Vega VB, Zhang W, Chen X *et al*. The Oct4 and Nanog transcription network regulates pluripotency in mouse embryonic stem cells. *Nat Genet* 2006; **38**: 431-440.

13 Reya T, Morrison SJ, Clarke MF, Weissman IL. Stem cells, cancer, and cancer stem cells. *Nature* 2001; **414**: 105-111.

14 Ben-Porath I, Thomson MW, Carey VJ, Ge R, Bell GW, Regev A *et al*. An embryonic stem cell-like gene expression signature in poorly differentiated aggressive human tumors. *Nat Genet* 2008; **40**: 499-507.

15 Niwa, H., Burdon T, Chambers I, Smith A. Self-renewal of pluripotent embryonic stem cells is mediated via activation of STAT3. *Genes Dev* 1998; **12**: 2048-2060.

16 Matsuda T, Nakamura T, Nakao K, Arai T, Katsuki M, Heike T *et al*. STAT3 activation is sufficient to maintain an undifferentiated state of mouse embryonic stem cells. *EMBO J* 1999; **18**: 4261-4269.

17 Yu H, Jove R. The STATs of cancer — new molecular targets come of age. *Nat Rev Cancer* 2004; **4**: 97-105.

18 Polakis P. Wnt signaling in cancer. *Cold Spring Harb Perspect Biol* 2012; **4**: a008052.

19 Sato N, Meijer L, Skaltsounis L, Greengard P, Brivanlou AH. Maintenance of pluripotency in human and mouse embryonic stem cells through activation of Wnt signaling by a pharmacological GSK-3-specific inhibitor. *Nat Med* 2004; **10**: 55-63.

20 Ogawa K, Nishinakamura R, Iwamatsu Y, Shimosato D, Niwa H. Synergistic action of Wnt and LIF in maintaining pluripotency of mouse ES cells. *Biochem Biophys Res Commun* 2006; **343**: 159-166.

21 Takao Y, Yokota T, Koide H. β-Catenin up-regulates Nanog expression through interaction with Oct-3/4 in embryonic stem cells. *Biochem Biophys Res Commun* 2007; **353**: 699-705.

22 Evangelista M., Tian H. & de Sauvage FJ. The hedgehog signaling pathway in cancer. *Clin Cancer Res* 2006; **12**: 5924-5928.

23 Ueda A. Involvement of Gli proteins in undifferentiated state maintenance and proliferation of embryonic stem cells. *J Juzen Med Soc* 2012; **121**: 38-46.

24 Schoonjans K, Dubuquoy L, Mebis J, Fayard E, Wendling O, Haby C *et al*. Liver receptor homolog 1 contributes to intestinal tumor formation through effects on cell cycle and inflammation. *Proc Natl Acad Sci USA* 2005; **102**: 2058-2062.

25 Jeter CR, Badeaux M, Choy G, Chandra D, Patrawala L, Liu C *et al*. Functional evidence that the self-renewal gene NANOG regulates human tumor development. *Stem Cells* 2009; **27**: 993-1005.

26 Li X, Ito M, Zhou F, Youngson N, Zuo X, Leder P *et al*. A maternal-zygotic effect gene, Zfp57, maintains both maternal and paternal imprints. *Dev Cell* 2008; **15**: 547-557.

27 Quenneville S, Verde G, Corsinotti A, Kapopoulou A, Jakobsson J, Offner S *et al*. In embryonic stem cells, ZFP57/KAP1 recognize a methylated hexanucleotide to affect

chromatin and DNA methylation of imprinting control regions. *Mol Cell* 2011; **44**: 361-372.

28 Chao W, D'Amore PA. IGF2: epigenetic regulation and role in development and disease. *Cytokine Growth Factor Rev* 2008; **19**: 111-120.

29 Pollak M. Insulin and insulin-like growth factor signalling in neoplasia. *Nat Rev Cancer* 2008; **8**: 915-928.

30 Akagi T, Usuda M, Matsuda T, Ko MS, Niwa H, Asano M *et al*. Identification of Zfp-57 as a downstream molecule of STAT3 and Oct-3/4 in embryonic stem cells. *Biochem Biophys Res Commun* 2005; **331**: 23-30.

31 Okazaki S, Tanase S, Choudhury BK, Setoyama K, Miura R, Ogawa M *et al*. A novel nuclear protein with zinc fingers down-regulated during early mammalian cell differentiation. *J Biol Chem* 1994; **269**: 6900-6907.

32 Alonso MB, Zoidl G, Taveggia C, Bosse F, Zoidl C, Rahman M *et al*. Identification and characterization of ZFP-57, a novel zinc finger transcription factor in the mammalian peripheral nervous system. *J Biol Chem* 2004; **279**: 25653-25664.

33 Zuo X, Sheng J, Lau HT, McDonald CM, Andrade M, Cullen DE *et al*. Zinc finger protein ZFP57 requires its co-factor to recruit DNA methyltransferases and maintains DNA methylation imprint in embryonic stem cells via its transcriptional

repression domain. *J Biol Chem* 2012; **287**: 2107-2118.

34 Mackay DJ, Callaway JL, Marks SM, White HE, Acerini CL, Boonen SE *et al*. Hypomethylation of multiple imprinted loci in individuals with transient neonatal diabetes is associated with mutations in ZFP57. *Nat Genet* 2008; **40**: 949-951.

35 Baglivo I, Esposito S, De Cesare L, Sparago A, Anvar Z, Riso V *et al*. Genetic and epigenetic mutations affect the DNA binding capability of human ZFP57 in transient neonatal diabetes type 1. *FEBS Lett* 2013; **587**: 1474-1481.

36 Gilmore AP. Anoikis. *Cell Death Differ* 2005; **12**: 1473-1477.

37 Taddei ML, Giannoni E, Fiaschi T, Chiarugi P. Anoikis: an emerging hallmark in health and diseases. *J Pathol* 2012; **226**: 380-393.

38 Cifone MA, Fidler IJ. Correlation of patterns of anchorage- independent growth with in vivo behavior of cells from a murine fibrosarcoma. *Proc Natl Acad Sci USA* 1980; **77**: 1039-1043.

39 Mori S, Chang JT, Andrechek ER, Matsumura N, Baba T, Yao G *et al*. Anchorage-independent cell growth signature identifies tumors with metastatic potential. *Oncogene* 2009; **28**: 2796-2805.

40 Samani AA, Yakar S, LeRoith D, Brodt P. The role of the IGF system in cancer growth and metastasis: overview and recent insights. *Endocr Rev* 2007; **28**: 20-47.

41 Lui JC, Baron J. Evidence that Igf2 down-regulation in postnatal tissues and up-regulation in malignancies is driven by transcription factor E2f3. *Proc Natl Acad Sci USA* 2013; **110**: 6181-6186.

42 Holm TM, Jackson-Grusby L, Brambrink T, Yamada Y, Rideout WM, Jaenisch R. Global loss of imprinting leads to widespread tumorigenesis in adult mice. *Cancer Cell* 2005; **8**: 275-285.

43 Jelinic P, Shaw P. Loss of imprinting and cancer. *J Pathol* 2007; **211**: 261-268.

44 Falix FA, Aronson DC, Lamers WH, Gaemers IC. Possible roles of DLK1 in the Notch pathway during development and disease. *Biochim Biophys Acta* 2012; **1822**: 988-995.

45 Royo H, Cavaillé J. Non-coding RNAs in imprinted gene clusters. *Biol Cell* 2008; **100**: 149-166.

46 Huarte M, Rinn JL. Large non-coding RNAs: missing links in cancer? *Hum Mol Genet* 2010; **19**: 152-161.

47 Farazi TA, Spitzer JI, Morozov P, Tuschl T. miRNAs in human cancer. *J Pathol* 2011; **223**: 102-115.

48 Takahashi K, Yamanaka S. Induction of pluripotent stem cells from mouse embryonic and adult fibroblast cultures by defined factors. *Cell* 2006; **126**: 663-676.

49 Yoshida-Koide U, Matsuda T, Saikawa K, Nakanuma Y, Yokota T, Asashima M *et al*. Involvement of Ras in extraembryonic endoderm differentiation of embryonic stem cells. *Biochem Biophys Res Commun* 2004; **313**: 475-481.

Figure Legends

Figure 1. ZFP57 is involved in anchorage-independent growth in HT1080 cells. (**a-c**) Overexpression of ZFP57 promotes anchorage-independent growth in HT1080 cells. HT1080 cells were transfected with either pCAGIP-myc (Control) or pCAGIP-myc-hZFP57(ZFP57), selected with puromycin, and subjected to soft agar assay. (**a**) Scanned images of HT1080 cell soft agar plates stained with MTT. Representative images of three independent experiments are shown. (**b**) The number of stained colonies was counted using the Image-J software. The number of colonies in control cells was set to 1.0, and data are shown as the mean ± standard deviation (n=3). *, $P<0.05$. (**c**) Western blot analysis using anti-myc antibody showing expression of myc-tagged human ZFP57 (Myc-ZFP57) in HT1080 cells. (**d**) Knockdown of ZFP57 inhibits anchorage-independent growth in HT1080 cells. HT1080 cells were transfected with pEBM-CAGIP-EmGFP-control miRNA, pEBM-CAGIP-EmGFP-ZFP57(349) or pEBM-CAGIP-EmGFP-ZFP57(427) and subjected to soft agar assay after puromycin selection. Error bars represent standard deviation [n=3 for ZFP57(349), n=4 for ZFP57(427)]. *, $P<0.05$.

Figure 2. ZFP57 is required for tumorigenicity in HT1080 cells *in vivo*. (**a**)

Knockdown of ZFP57 reduces HT1080 tumor growth in nude mice. HT1080/pCALiPL-ZFP57(427) cells were pretreated with ethanol vehicle (EtOH) or 4-HT and injected subcutaneously into mice. Note that 4-HT pretreatment results in suppression of endogenous ZFP57 in HT1080/pCALiPL-ZFP57(427) cells. (**b**) Overexpression of ZFP57 promotes HT1080 tumor formation in nude mice. HT1080 cells were transfected with pCAGIP-myc (Control) or pCAGIP-myc-hZFP57(ZFP57), and puromycin-resistant clones were injected subcutaneously. In both experiments, mice were sacrificed 2 weeks after injection, and tumor volume was measured. Median values are represented by horizontal bars. *, $P<0.05$ by Mann-Whitney test.

Figure 3. ZFP57 regulates IGF2 expression. (**a**) ZFP57 binds to IGF2-H19 ICR *in vivo*. HT1080 cells transfected with either pCAGIP-Flag (Control) or pCAGIP-Flag-hZFP57 (ZFP57) were subjected to ChIP assay using anti-flag antibody with primers specific for the ZFP57-binding region of the IGF2-H19 ICR. Data shown are representative data of three separate experiments. (**b**) IGF2 expression is downregulated by knockdown of ZFP57. HT1080 cells constitutively expressing either control or ZFP57 miRNA were generated by transfecting pEBM-CAGIP constructs, and IGF2 and ZFP57 mRNA expression levels were measured by

quantitative RT-PCR. The expression levels of IGF2 and ZFP57 in control cells were set to 1.0. Error bars indicate standard deviation in triplicate samples. *, $P<0.05$. Representative data of three independent experiments are shown.

Figure 4. IGF2 is required for anchorage-independent growth in HT1080 cells. (**a**) The IGF1 receptor is expressed in HT1080 cells. Expression of the IGF1 receptor (IGF1r) was examined by Western blot analysis. HEK293 cells were used as a positive control. (**b**) IGF2 induces the activation of AKT. HT1080 cells were starved overnight in serum-free medium supplemented with 0.1% bovine serum albumin, and then stimulated for 15 min with recombinant IGF2 protein (100ng/ml) (Bay bioscience, Kobe, Japan). (c) ZFP57 knockdown reduces AKT phosphorylation. HT1080 cells transfected with either control vector or ZFP57 miRNA-expression vector were cultured in the presence of 10% fetal bovine serum for 3 days. In both experiments, cells were harvested, lysed, and subjected to Western blot analysis. Representative data from three independent experiments are shown. (**d**) IGF2 neutralizing antibody suppresses anchorage-independent growth in HT1080 cells. Neutralizing antibody was added to the top layer at the concentration of 10 μg/ml. (**e**) IGF2 neutralization abolishes ZFP57-mediated growth in soft agar. HT1080 cells

were transfected with ZFP57 and subjected to soft agar assay in the presence or absence of the IGF2 neutralizing antibody. In both experiments, the number of colonies in control cells was set to 1.0, and error bars represent standard deviation (n=3). *, $P<0.05$. (**f**) Knockdown of IGF2 reduces HT1080 tumor growth in nude mice. HT1080 cells were transfected with pEBM-CAGIP-EmGFP-IGF2(779), and puromycin-resistant clones were injected into nude mice subcutaneously. Mice were sacrificed 2 weeks after injection, and tumor volume was measured. (**g**) IGF2 knockdown attenuates the enhanced tumor growth due to Zfp57 overexpression. HT1080 cells expressing IGF2 miRNA were transfected with pCAGIH3-mZfp57, and hygromycin-resistant clones were injected subcutaneously. Mice were sacrificed 9 days after injection to measure tumor volume. In both experiments, median values are represented by horizontal bars. *, $P<0.05$ by Mann-Whitney test.

Figure 5. Zfp57 is involved in anchorage-independent growth in ES cells. 1F9 cells [Zfp57(+/-)] and 2E9 cells [Zfp57(-/-)] were subjected to soft agar assay. (**a**) Representative scans of ES cell soft agar plates stained with MTT. (**b**) The number of stained colonies was counted using the Image-J software. The colony number in 1F9 ES cells was set to 1.0. Error bars represent standard deviation (n=4). *, $P<0.05$.

Figure 6. Overexpression of ZFP57 induces anchorage-independent growth in NIH3T3 cells. NIH3T3 cells were transfected with pCAGIP-myc (Control) or pCAGIP-myc-hZFP57 (ZFP57), and subjected to soft agar assay. (**a**) Representative scans of NIH3T3 cell soft agar plates stained with MTT. (**b**) The number of stained colonies was counted using the Image-J software. Error bars represent standard deviation (n=3). *, $P<0.05$. (**c**) Western blot analysis using anti-myc antibody showing myc-tagged human ZFP57 expression in NIH3T3 cells.

Figure 7. ZFP57 is overexpressed in tumor tissues.

Immunohistochemical staining of ZFP57 expression in pancreatic (**a**) and esophageal (**b**) tumors and normal tissues. Representative images are shown. The arrows indicate ZFP57-positive cells.

Table I. ZFP57 overexpression in tumor specimens from cancer patients.

Primary site (carcinoma)	No. of patients	No. of ZFP57-positive (%)
Pancreatic cancer	15	11 (73%)
Gastric cancer	20	9 (45%)
Breast cancer	20	8 (40%)
Colorectal cancer	20	8 (40%)
Esophageal cancer	20	7 (35%)
Hepatocellular carcinoma	20	1 (5.0%)
Cholangiocellular carcinoma	20	1 (5.0%)

Figure 1 Tada Y *et al.*

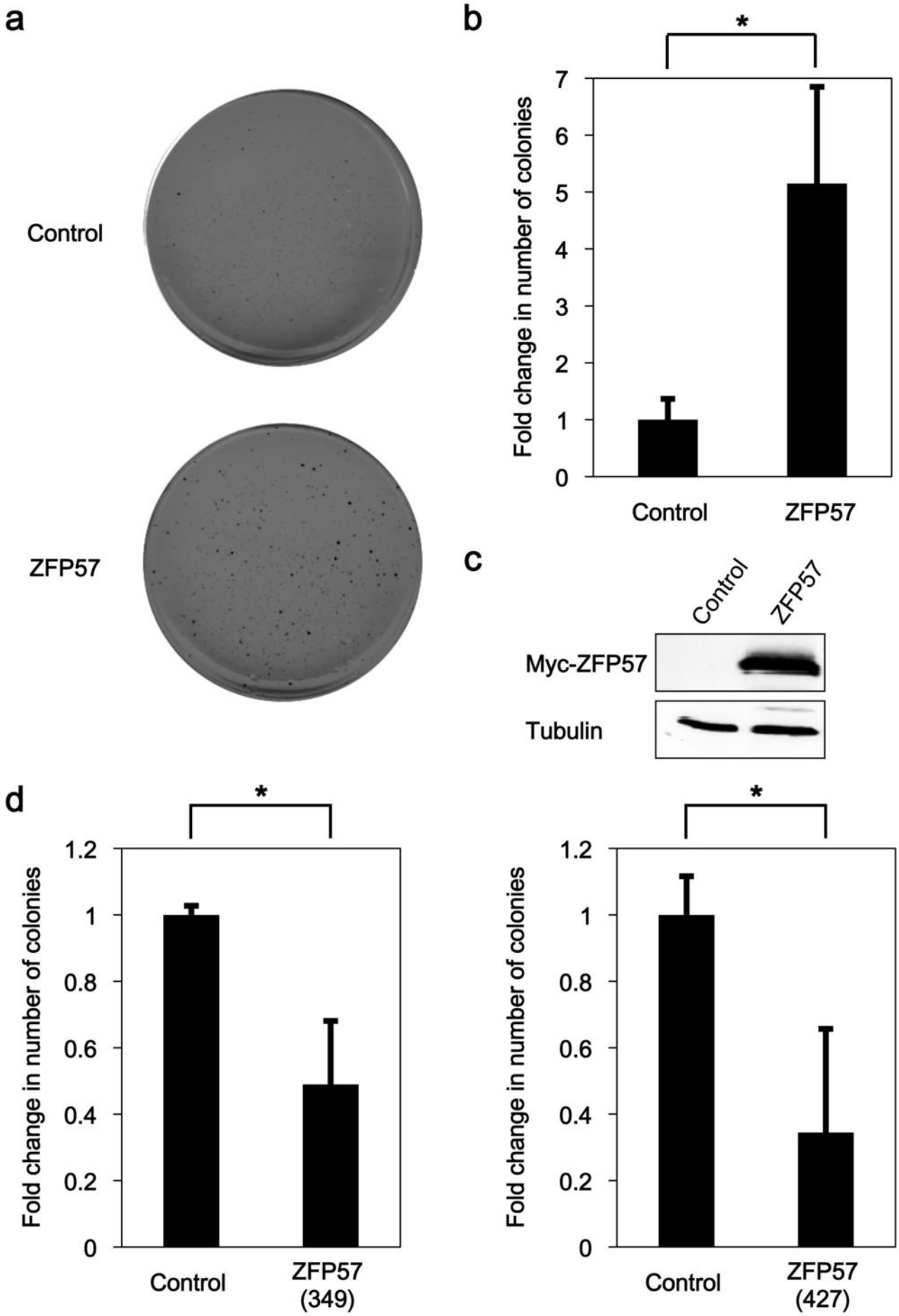

Figure 2 Tada Y *et al.*

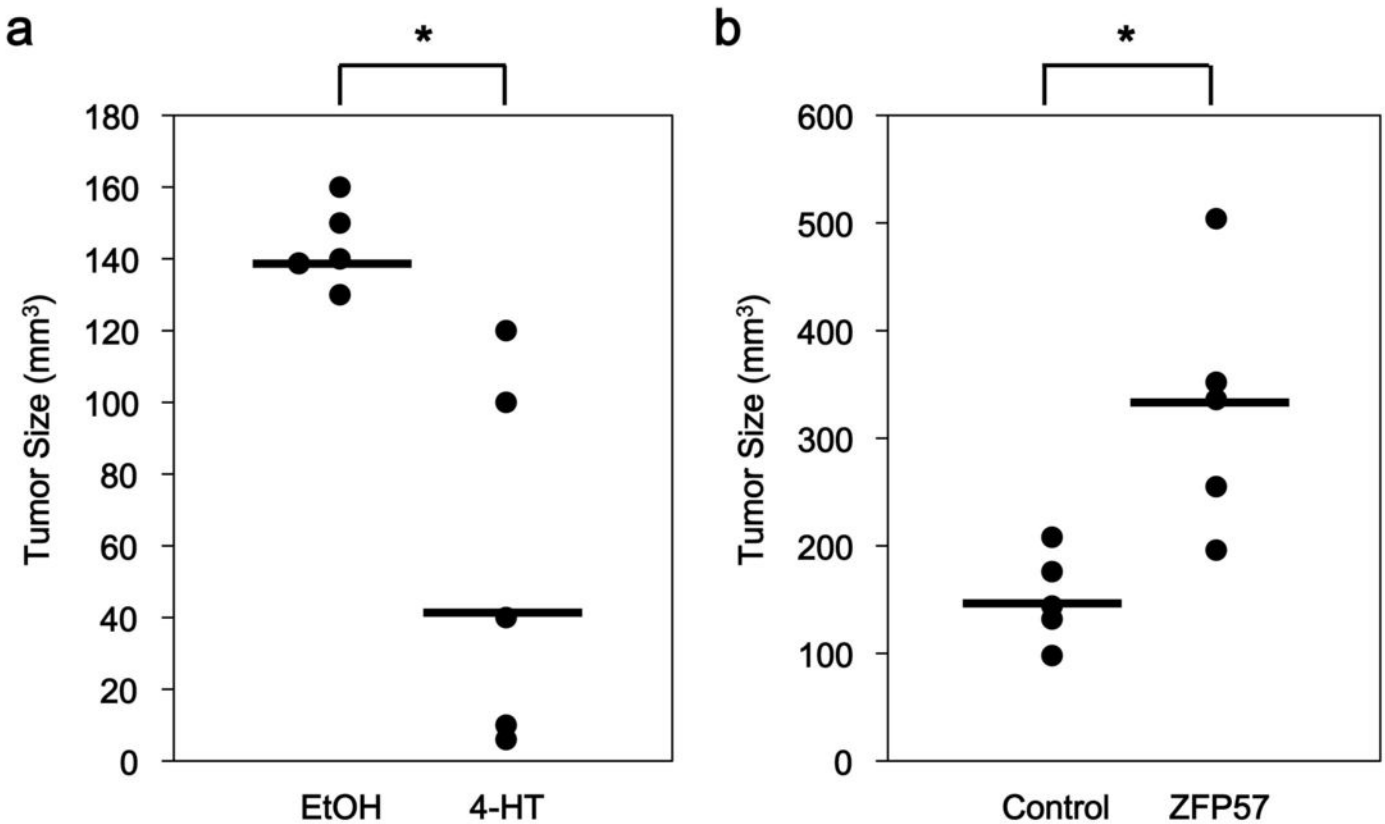

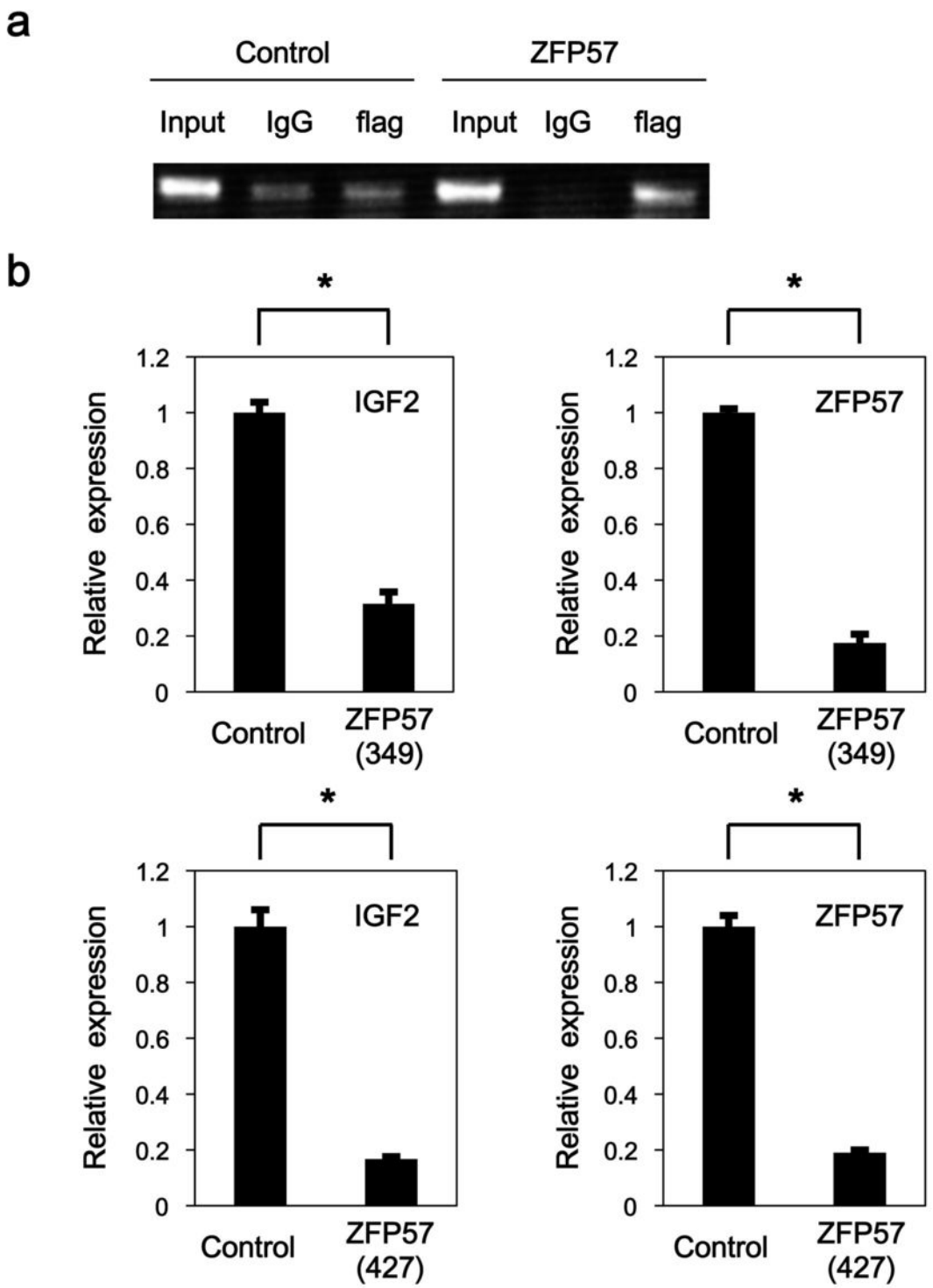
a
Control
ZFP57
Input
IgG
flag
Input
IgG
flag
b
*
IGF2
Relative expression
1.2
1
0.8
0.6
0.4
0.2
0
Control
ZFP57 (349)
*
ZFP57
Relative expression
Control
ZFP57 (349)
*
IGF2
Relative expression
Control
ZFP57 (427)
*
ZFP57
Relative expression
Control
ZFP57 (427)

Figure 4 Tada Y *et al.*

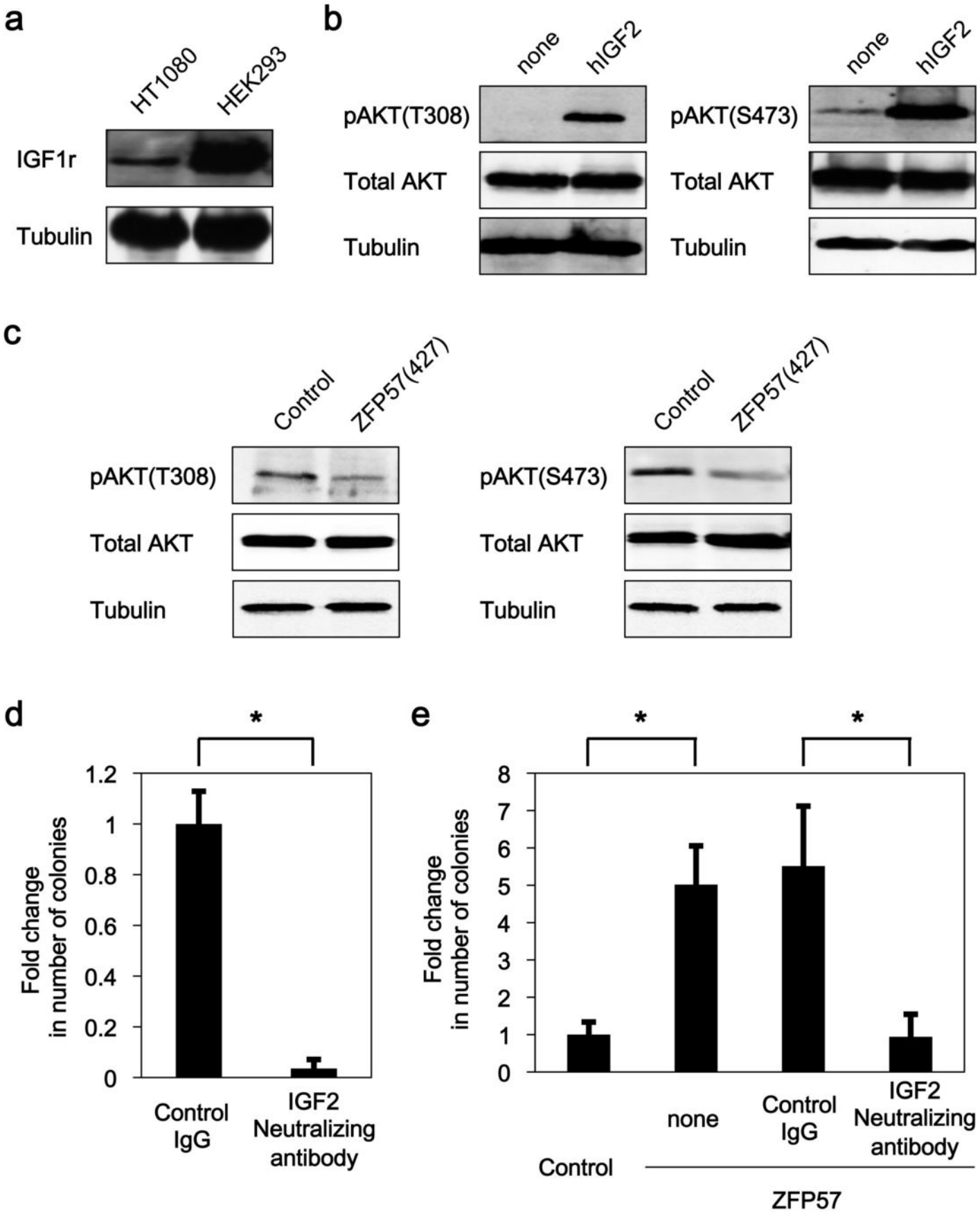

Figure 4 Tada Y *et al.*

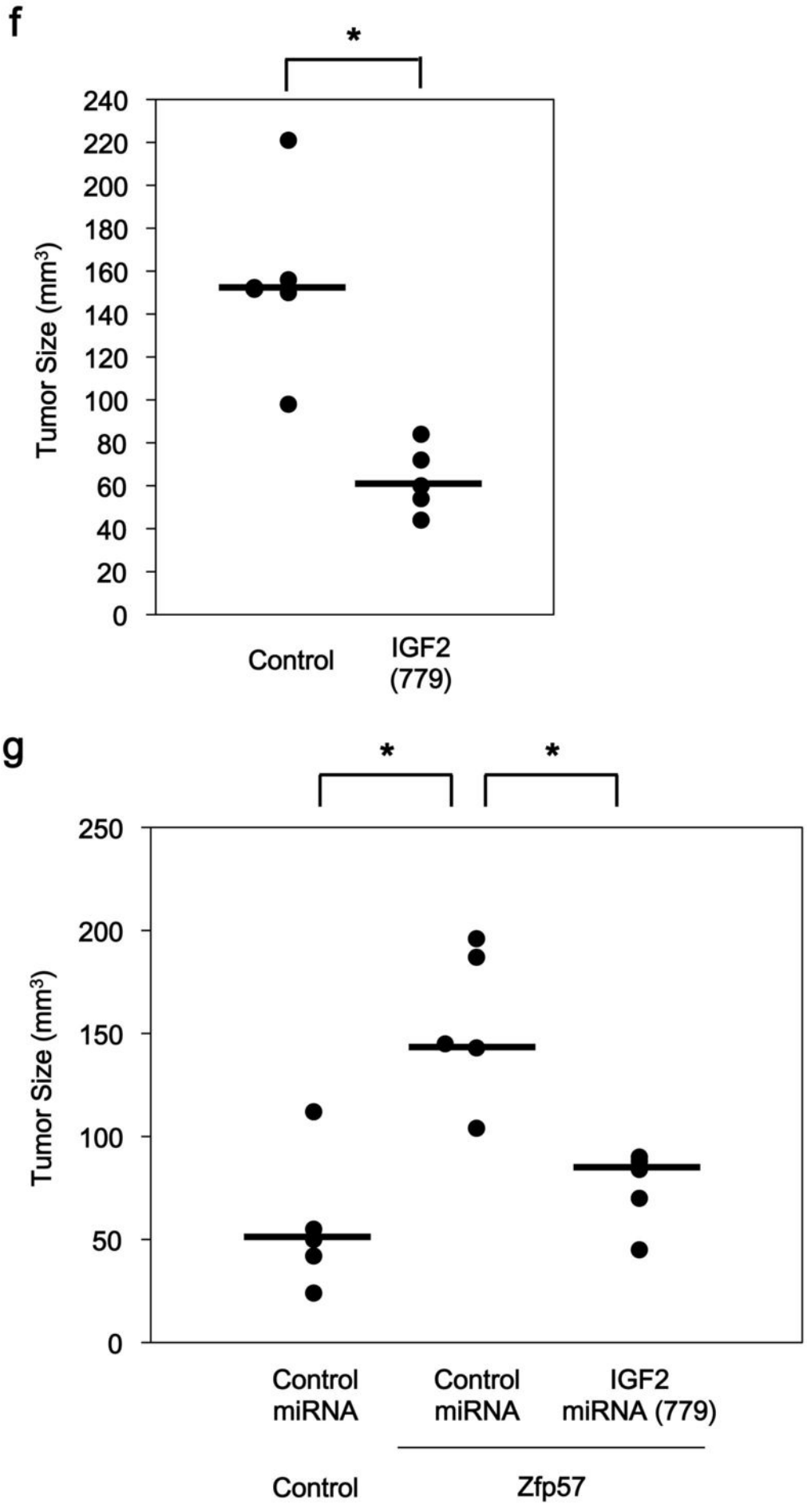

Figure 5 Tada Y *et al.*

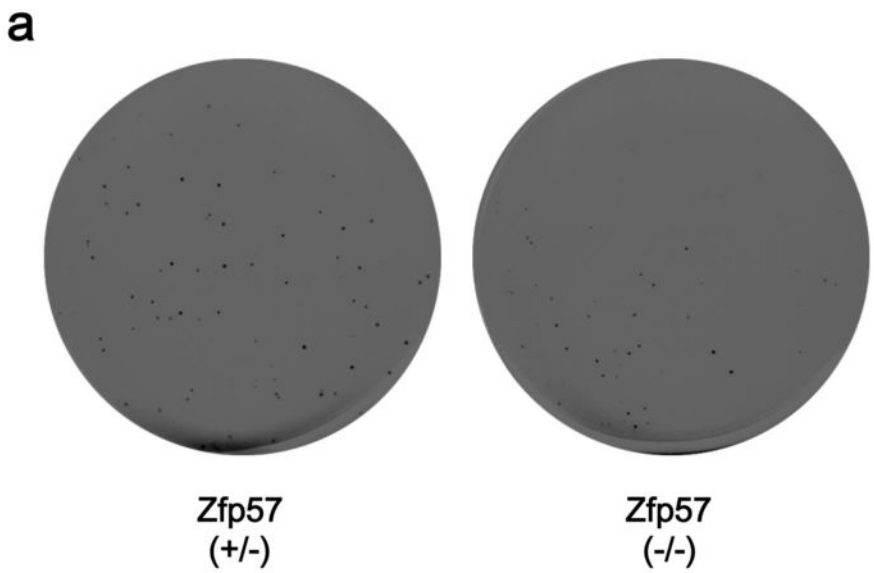

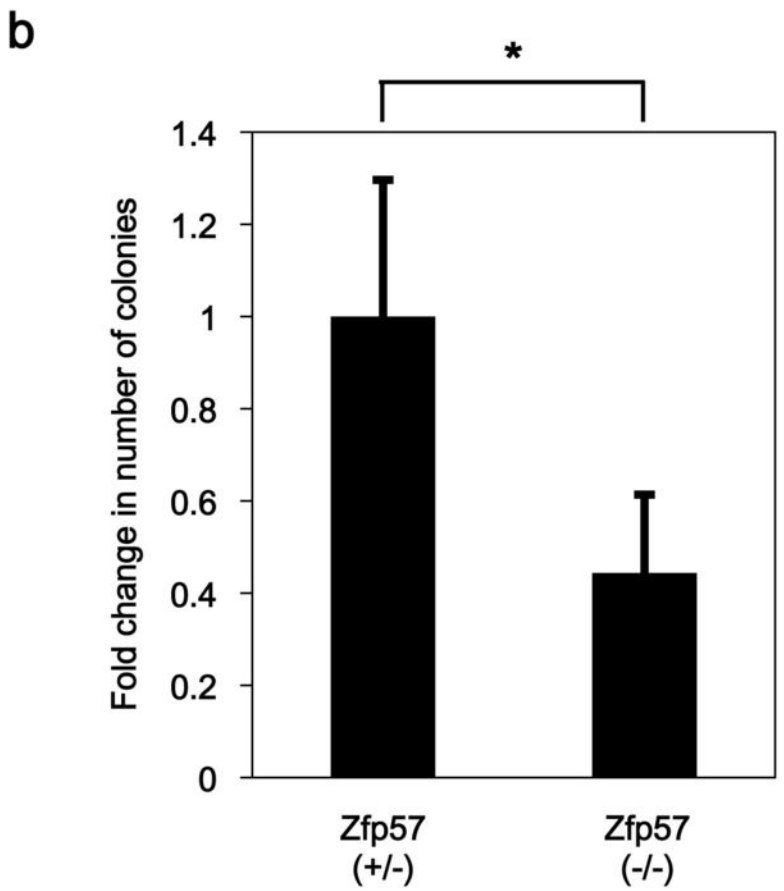

Figure 6 Tada Y *et al.*

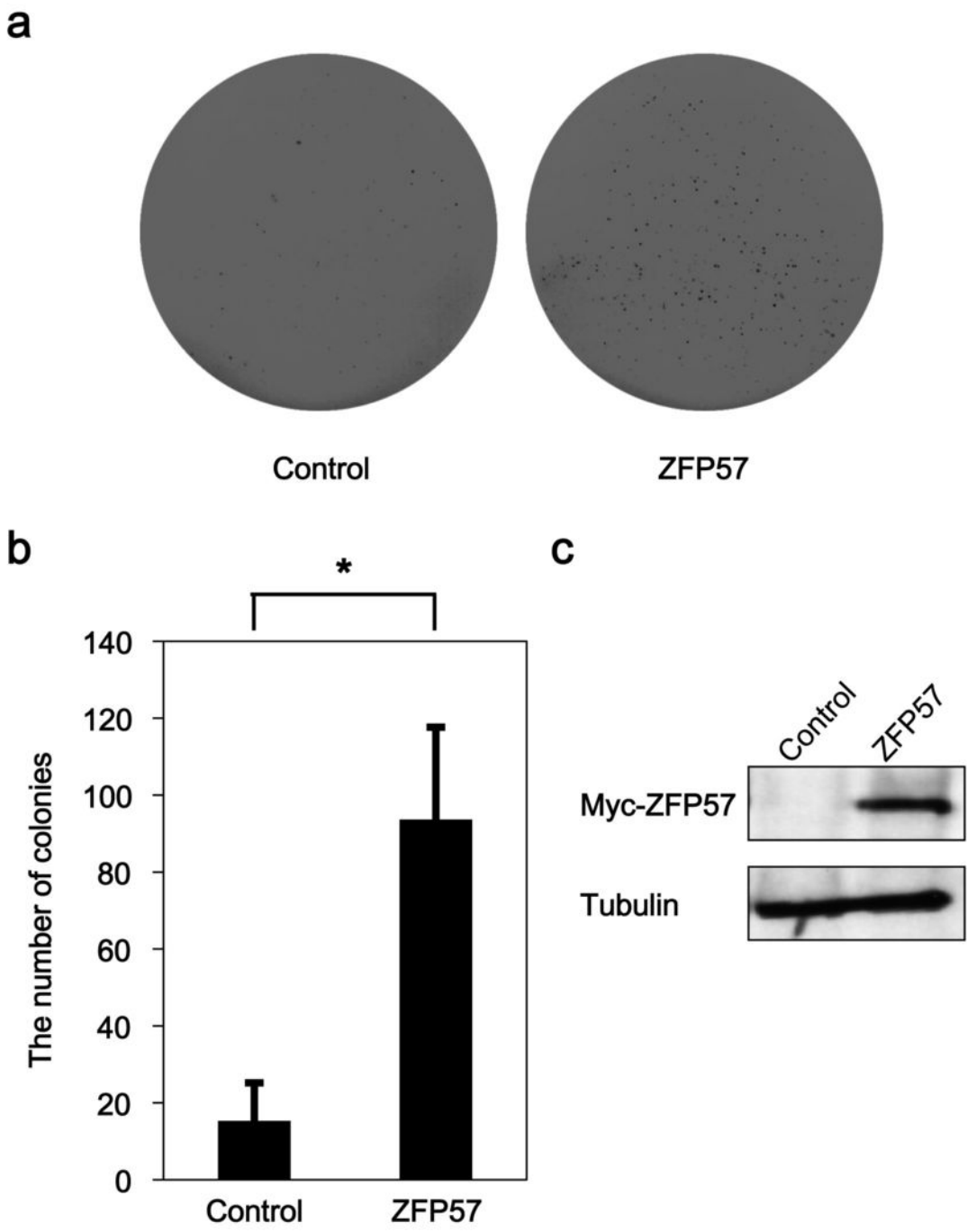

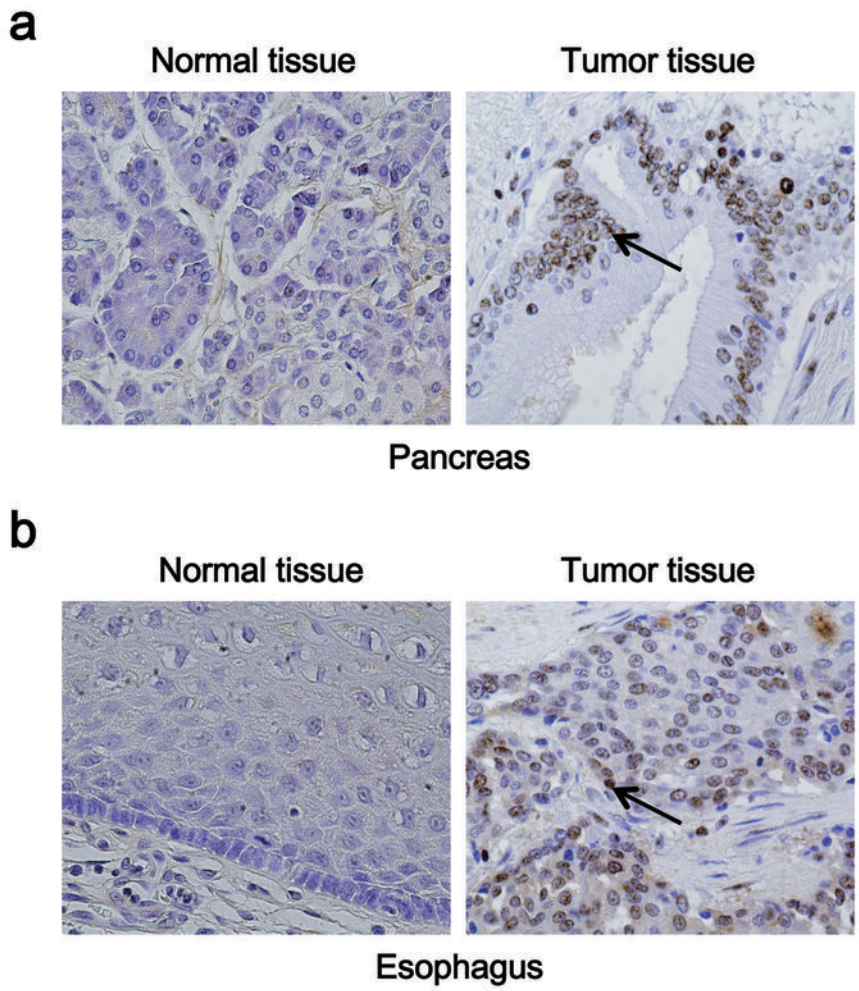
a
Normal tissue
Tumor tissue
Pancreas
b
Normal tissue
Tumor tissue
Esophagus

Supplementary Information

"The stem cell transcription factor ZFP57 induces IGF2 expression to promote anchorage-independent growth in cancer cells." by Tada, Y. *et al.*

Table S1 Sequences of used primers and oligonucleotides

Primers for cloning		
Gene Name	Forward Primer (5' to 3')	Reverse Primer (5' to 3')
human ZFP57	GATATCATGTTTGAACAGCTGAAGCC	GCGGCCGCTTATTTATGTTTCAAGATGC
mouse Zfp57	GAATTCATGGCAGCTAGGAAACAGTCTTCC	GCGGCCGCTCAGTCCGAATCTTCTTC
Primers for regular RT-PCR and quantitative RT-PCR		
Gene Name	Forward Primer (5' to 3')	Reverse Primer (5' to 3')
human ZFP57	AAGCCAGAGGTCCATCCAG	GGGCAACAGAAGACATTGAG
IGF2	GTGGCATCGTTGAGGAGTG	GGGTGGGTAGAGCAATCAGG
β-actin	AAACTGGAACGGTGAAGGTG	GTGGACTTGGGAGAGGACTG
mouse Zfp57	GAATTCTGTAATTTCTGTGGCAAGAC	GCGGCCGCTGTGGATCTTGAGGTGGGTTAA
G3PDH	ACCACAGTCCATGCCATCAC	TCCACCACCCTGTTGCTGTA
Primers for ChIP analysis		
Gene Name	Forward Primer (5' to 3')	Reverse Primer (5' to 3')
IGF2-H19 ICR	TGGCAGGCACAGAAACTG	GAGCGTCCTATTCCCAGAAG
Oligonucleotides for miRNA vector construction		
Gene Name	Forward Primer (5' to 3')	Reverse Primer (5' to 3')
ZFP57(349)	TGCTGATAACATCCTGGTAAAGGACCGTTTTGGCCACTGACTGACGGTCCTTTCAGGATGTTAT	CCTGATAACATCCTGAAAGGACCGTCAGTCAGTGGCCAAAACGGTCCTTTACCAGGATGTTATC
ZFP57(427)	TGCTGTGCTCAAGCTTGGTGATTAGCGTTTTGGCCACTGACTGACGCTAATCAAAGCTTGAGCA	CCTGTGCTCAAGCTTTGATTAGCGTCAGTCAGTGGCCAAAACGCTAATCACCAAGCTTGAGCAC
IGF2(779)	TGCTGAAGAAGGTGAGAAGCACCAGCGTTTTGGCCACTGACTGACGCTGGTGCCTCACCTTCTT	CCTGAAGAAGGTGAGGCACCAGCGTCAGTCAGTGGCCAAAACGCTGGTGCTTCTCACCTTCTTC

Legends for supplementary figures

Figure S1. Search for ES-specific genes that promote anchorage-independent growth in HT1080 cells. HT1080 cells were transfected with either an empty vector or expression vectors encoding the indicated genes, which were cloned from mouse ES cells. Puromycin-resistant clones were then pooled and subjected to soft agar assay. Black and gray bars show the data of the 1st and 2nd experiments, respectively. The numbers of colonies in control cells were set to 1.0 (indicated by red line). The expression vector for Klf4 was kindly provided by Dr. Hitoshi Niwa.

Figure S2. Overexpression of Zfp57 recovers the reduced anchorage-independent growth of ZFP57 knockdown HT1080 cells. (**a**) Soft agar assay. HT1080 cells expressing ZFP57 miRNA(427) were transfected with empty vector (control) or pCAGIN3-myc-mZfp57 (Zfp57), and selected by the presence of G418. Resistant clones were then subjected to soft agar assay. The number of stained colonies in control cells was set to 1.0. Error bars represent standard deviation (n=3). *, $P<0.05$. (**b**) Expression of exogenous mouse Zfp57 was confirmed by regular RT-PCR. Glyceraldehyde 3-phosphate dehydrogenase (G3PDH) was used as an internal control.

Primers used for RT-PCR are listed in Supplementary Table S1.

Figure S3. Establishment of HT1080/pCALiPL-ZFP57(427) cells. (**a**) Strategy of inducible ZFP57 knockdown. Since HT1080/pCALiPL-ZFP57(427) cells express ER-Cre-ER, a fusion protein between Cre recombinase and the ligand-binding domain of the estrogen receptor, 4-hydroxytamoxifen (4-HT) treatment stimulates Cre-mediated recombination, leading to deletion of the region between loxP sites. As a result, expression of EmGFP and ZFP57 miRNA is induced. (**b**) Treatment with 4-HT reduces ZFP57 expression in HT1080/pCALiPL-ZFP57(427) cells. HT1080/pCALiPL-ZFP57 miRNA cells were cultured in the presence of ethanol vehicle (EtOH) or 1 μM 4-HT, and subjected to quantitative RT-PCR. The expression level of ZFP57 in control cells (*i.e.,* ethanol-treated cells) was set to 1.0. Error bars indicate standard deviation in triplicate samples. *, $P<0.05$. Representative data from three independent experiments are shown. (**c**) Knockdown of ZFP57 reduces the anchorage independence of HT1080 cells. HT1080/pCALiPL-ZFP57 miRNA cells were subjected to soft agar assay in the presence of ethanol vehicle (EtOH) or 4-HT. The number of stained colonies in control cells was set to 1.0. Error bars represent standard deviation (n=3). *, $P<0.05$.

Figure S4. ZFP57 expression in resulting tumors. RNA was prepared from three control HT1080-derived tumors and three ZFP57-overexpressing HT1080-derived tumors and subjected to quantitative RT-PCR to determine the expression level of ZFP57 in each tumor. The expression level of ZFP57 in control cells (#1) was set to 1.0. Error bars indicate standard deviation in triplicate samples.

Figure S5. Overexpression of Zfp57 rescues the reduced IGF2 expression in ZFP57 knockdown HT1080 cells. (**a**) Recovery of IGF2 expression by Zfp57 overexpression. After transfection with empty vector (control) or pCAGIH3-mZfp57 (Zfp57), ZFP57 knockdown HT1080 cells were subjected to quantitative RT-PCR to determine the expression level of IGF2. The expression level of IGF2 in control cells was set to 1.0. Error bars indicate standard deviation in triplicate samples. *, $P<0.05$. (**b**) Confirmation of exogenous mouse Zfp57 expression by regular RT-PCR.

Figure S6. IGF2 is required for anchorage-independent growth in HT1080 cells. (**a**) Knockdown of IGF2 inhibits anchorage-independent growth in HT1080 cells. Error bars represent standard deviation (n=3). *, $P<0.05$. (**b**) Downregulation of IGF2

expression upon IGF2 knockdown. The expression level of IGF2 in control cells was set to 1.0. Error bars indicate standard deviation in triplicate samples. *, $P<0.05$. Representative data from three independent experiments are shown. HT1080 cells were transfected with pEBM-CAGIP-EmGFP-control or pEBM-CAGIP-EmGFP-IGF2(779), and subjected to soft agar assay and quantitative RT-PCR after puromycin selection.

Figure S7. Zfp57 expression in HT1080 transfectants. HT1080 transfectants were subjected to regular RT-PCR to confirm the expression of exogenous mouse Zfp57.

Figure S8. Zfp57 overexpression restores the reduced anchorage-independent growth of *Zfp57*-null ES cells. (**a**) 1F9 cells and 2E9 cells were transfected with empty vector (control) or pCAGIP-myc-Zfp57 (Zfp57). After selection with puromycin, cells were subjected to soft agar assay. The number of colonies in 1F9 cells was set to 1.0, and error bars represent standard deviation (n=3). *, $P<0.05$. (**b**) Expression of endogenous and exogenous mouse ZFP57 protein. Cell lysates were subjected to immunoblot analysis with an antibody against mouse ZFP57 antibody.[30] Note that myc-tagged ZFP57 shows slightly slower mobility than endogenous ZFP57.

Figure S9. Western blotting analysis of ZFP57. Cell lysates were prepared from HEK293 cells transfected with either control vector (control) or pCAGIP-HA-hZFP57 (hZFP57) and subjected to Western blot analysis with anti-hZFP57 antibody (upper panel) and anti-α-tubulin antibody (lower panel).

Figure S10. Immunohistochemical staining of IGF2 expression in breast (**a**) and esophageal (**b**) tumors and normal tissues. Representative images are shown.

Figure S1

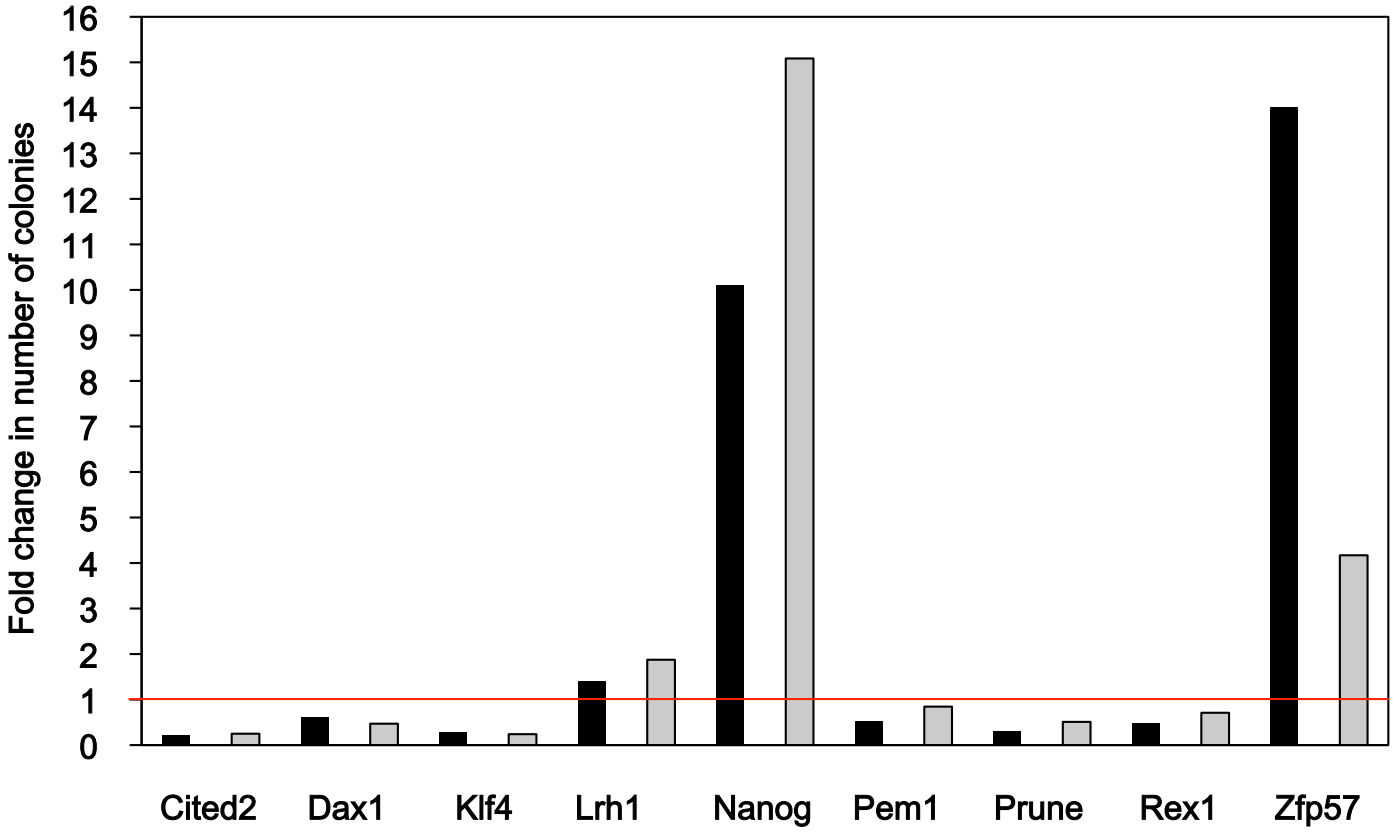
Fold change in number of colonies
16
15
14
13
12
11
10
9
8
7
6
5
4
3
2
1
0
Cited2
Dax1
Klf4
Lrh1
Nanog
Pem1
Prune
Rex1
Zfp57

Figure S2

a

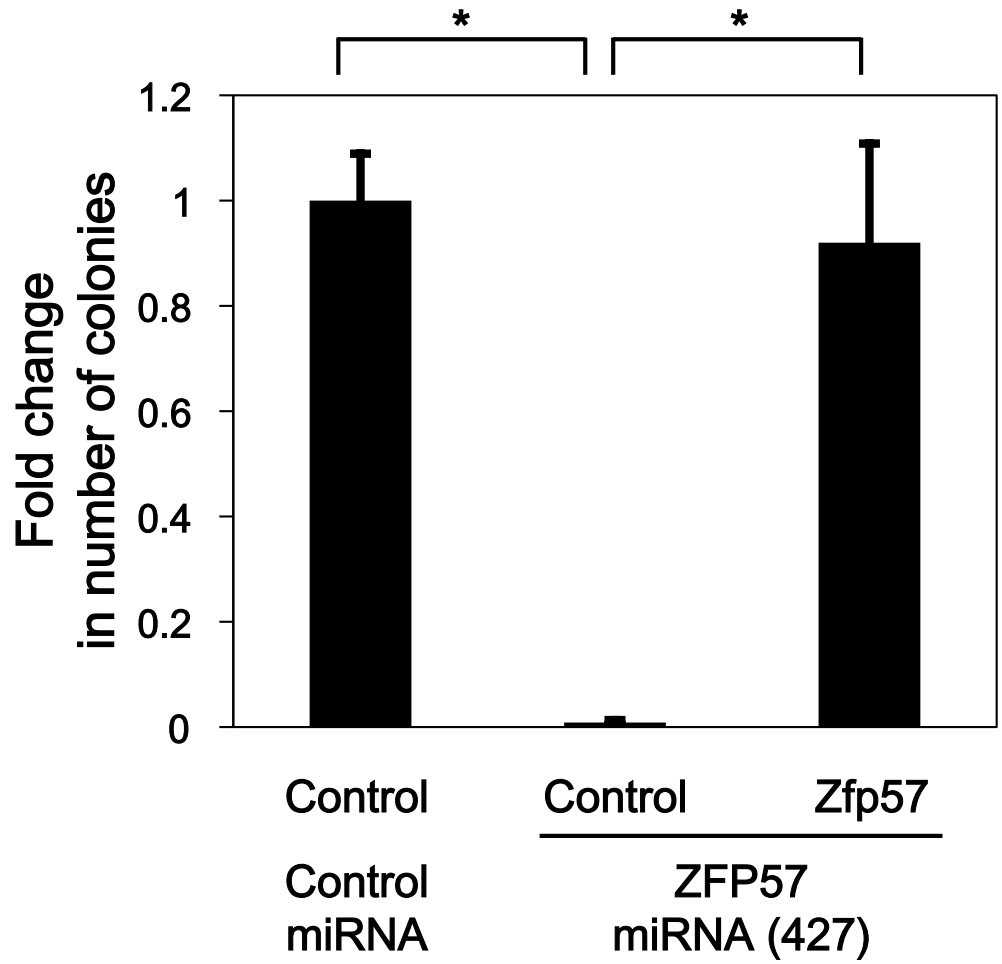
*
*
1.2
1
0.8
0.6
0.4
0.2
0
Fold change
in number of colonies
Control
Control
Zfp57
Control
miRNA
ZFP57
miRNA (427)

b

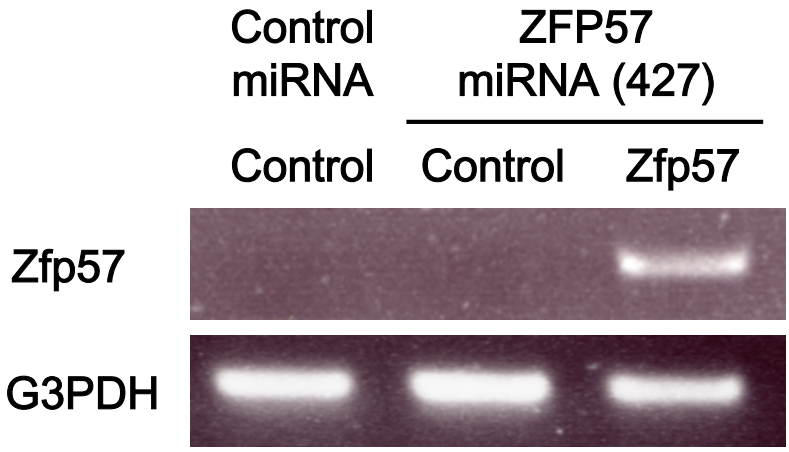
Control
miRNA
ZFP57
miRNA (427)
Control
Control
Zfp57
Zfp57
G3PDH

Figure S3

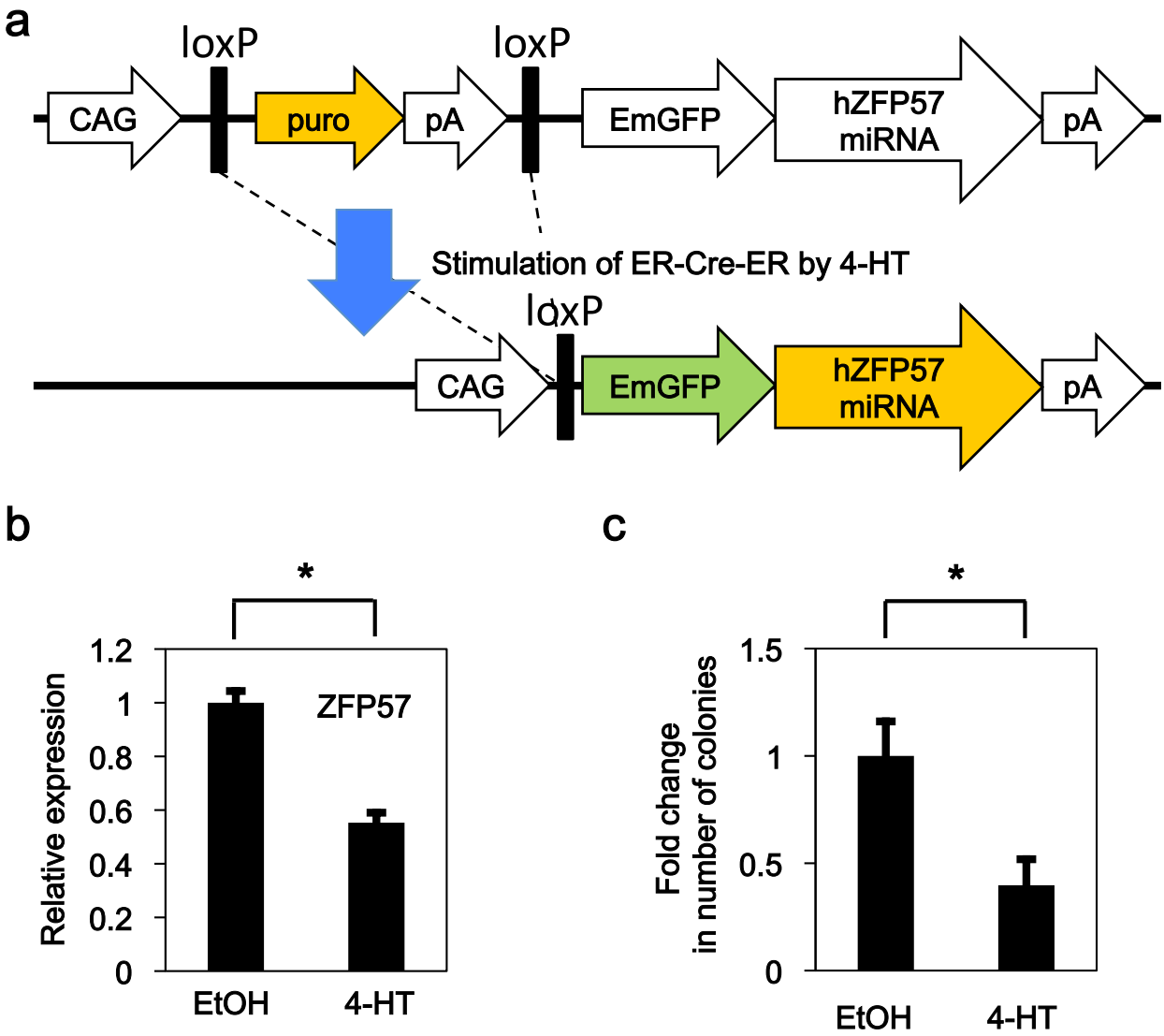
a
loxP
loxP
CAG
puro
pA
EmGFP
hZFP57
miRNA
pA
Stimulation of ER-Cre-ER by 4-HT
loxP
CAG
EmGFP
hZFP57
miRNA
pA
b
*
Relative expression
1.2
1
0.8
0.6
0.4
0.2
0
ZFP57
EtOH
4-HT
c
*
Fold change
in number of colonies
1.5
1
0.5
0
EtOH
4-HT

Figure S4

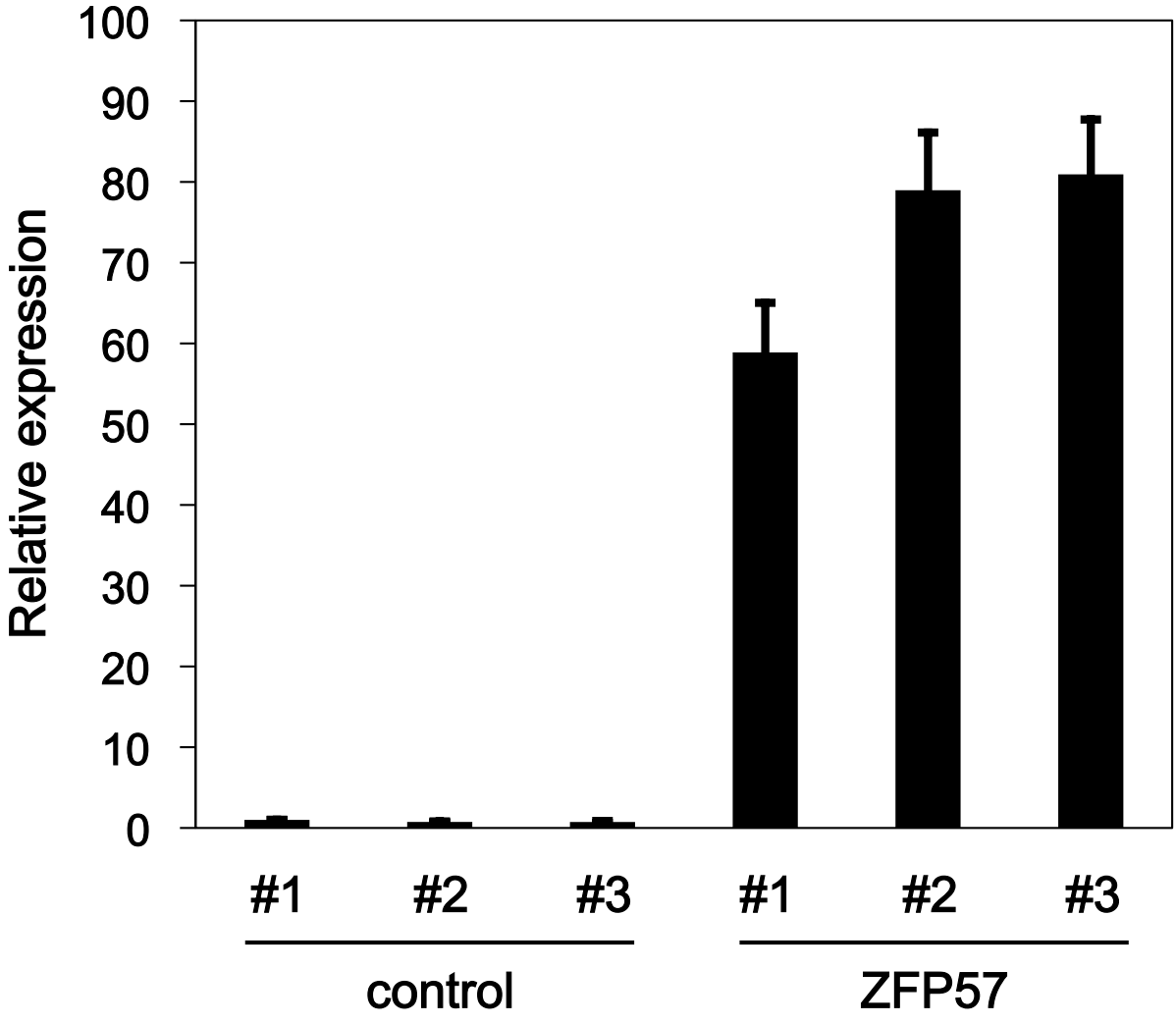
Relative expression
100
90
80
70
60
50
40
30
20
10
0
#1
#2
#3
#1
#2
#3
control
ZFP57

Figure S5

a

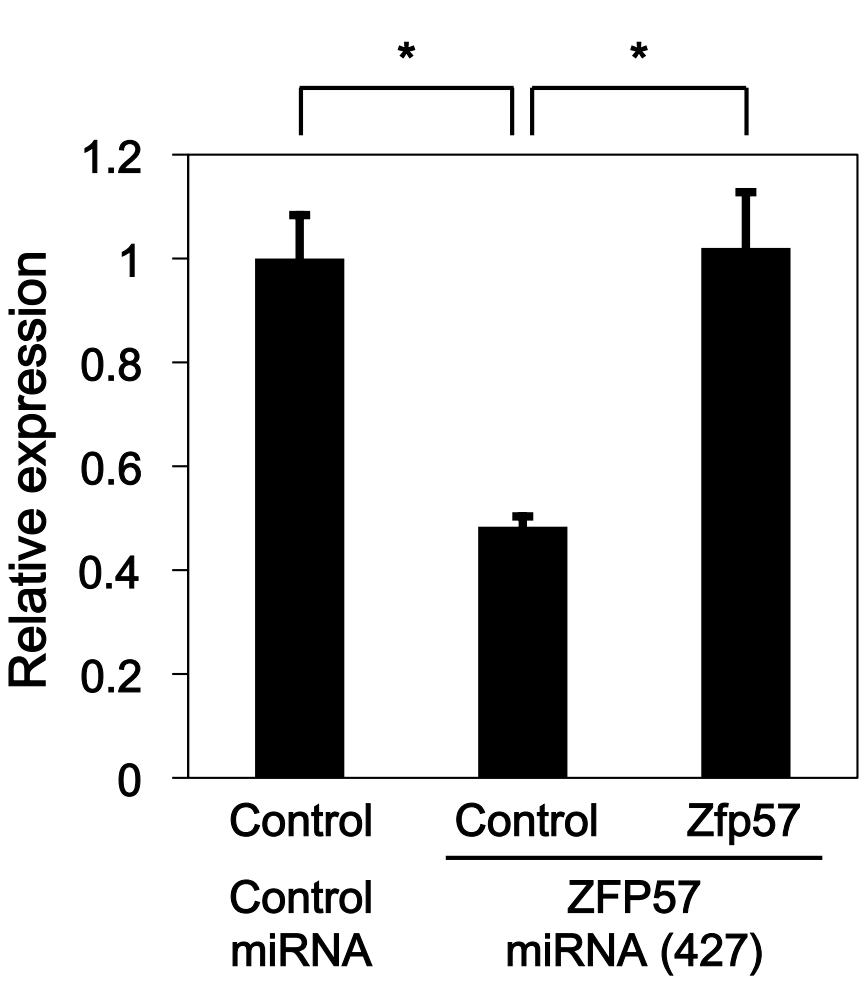
*
*
1.2
1
0.8
0.6
0.4
0.2
0
Relative expression
Control
Control
Zfp57
Control miRNA
ZFP57 miRNA (427)

b

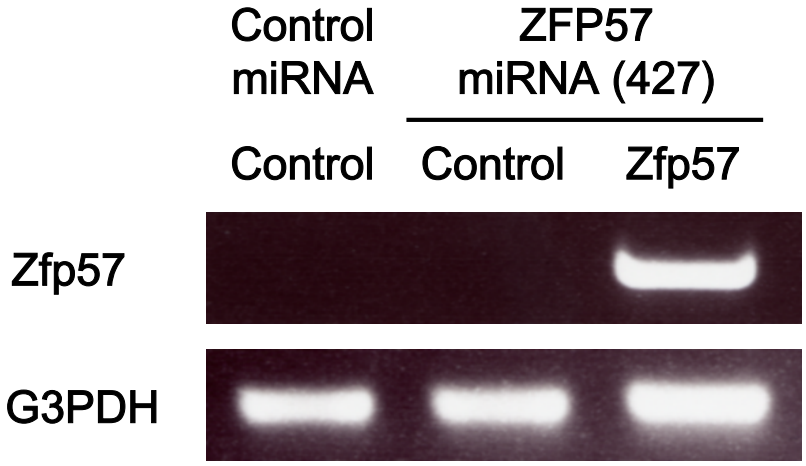
Control miRNA
ZFP57 miRNA (427)
Control
Control
Zfp57
Zfp57
G3PDH

Figure S6

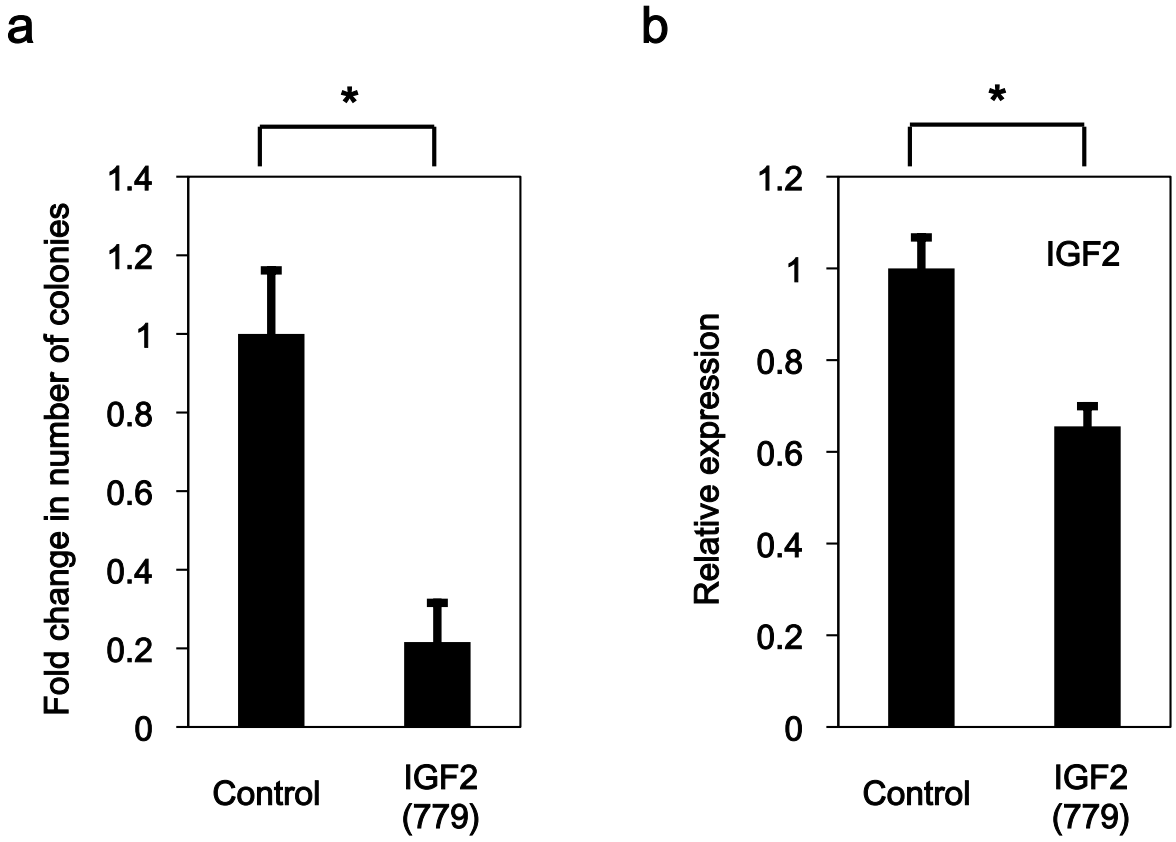
a
*
1.4
1.2
1
0.8
0.6
0.4
0.2
0
Fold change in number of colonies
Control
IGF2
(779)
b
*
1.2
1
0.8
0.6
0.4
0.2
0
Relative expression
IGF2
Control
IGF2
(779)

Figure S7

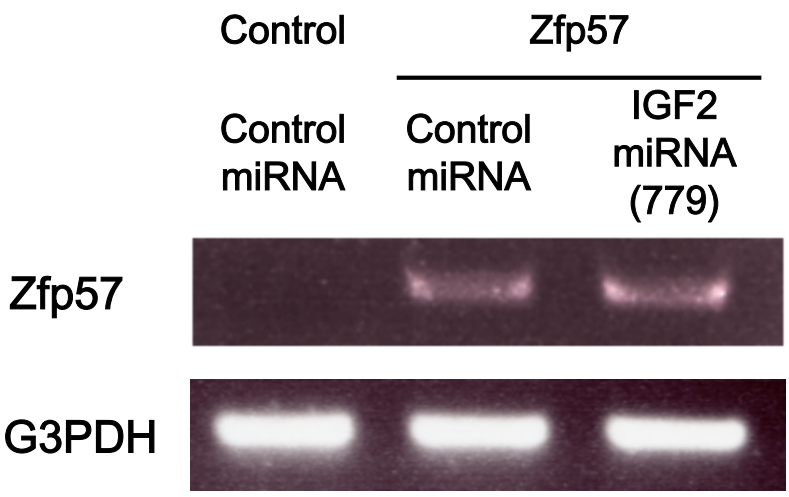
Control
Zfp57
Control miRNA
Control miRNA
IGF2 miRNA (779)
Zfp57
G3PDH

Figure S8

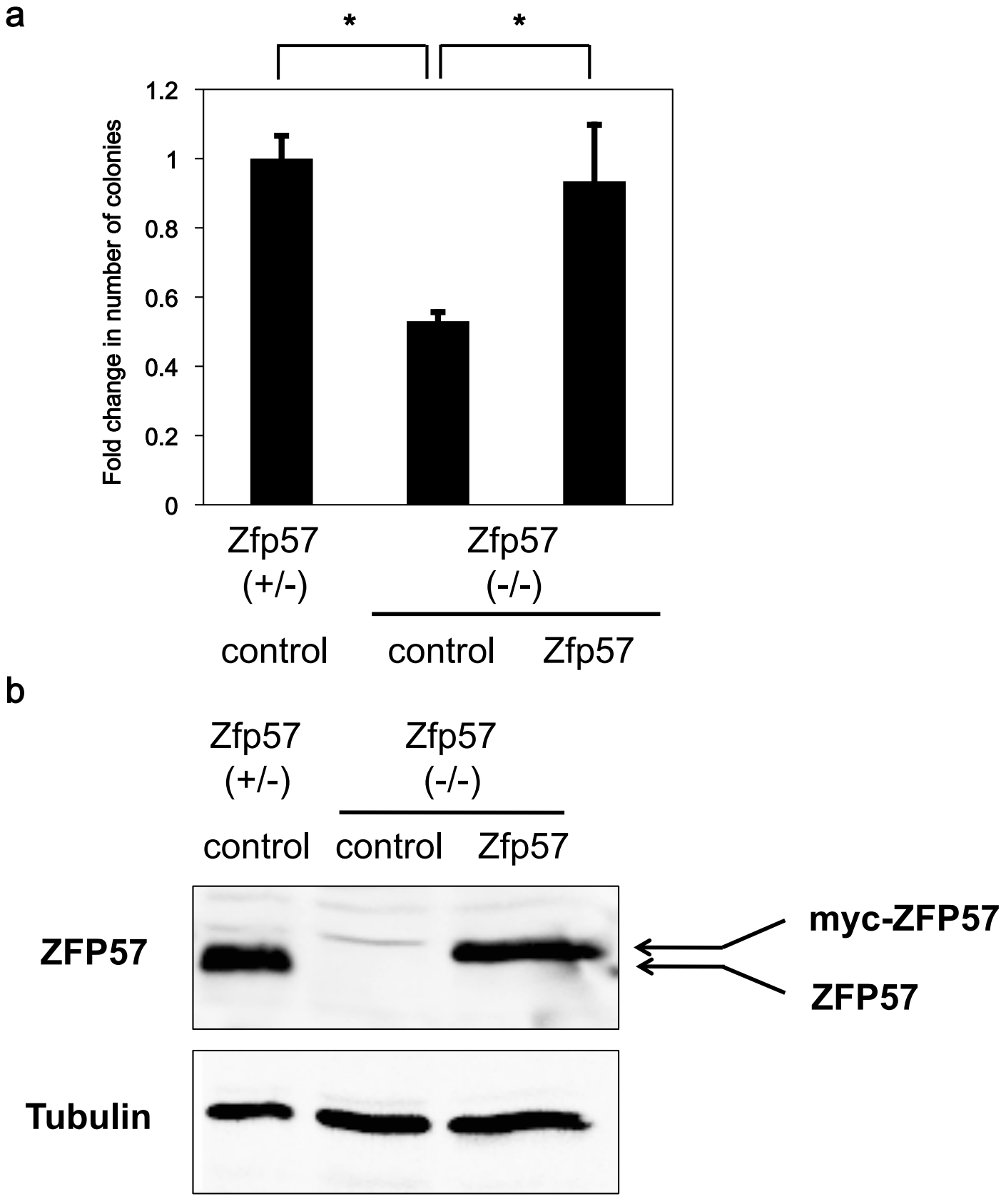
a
*
*
1.2
1
0.8
0.6
0.4
0.2
0
Fold change in number of colonies
Zfp57
(+/-)
Zfp57
(-/-)
control
control
Zfp57
b
Zfp57
(+/-)
Zfp57
(-/-)
control
control
Zfp57
ZFP57
myc-ZFP57
ZFP57
Tubulin

Figure S9

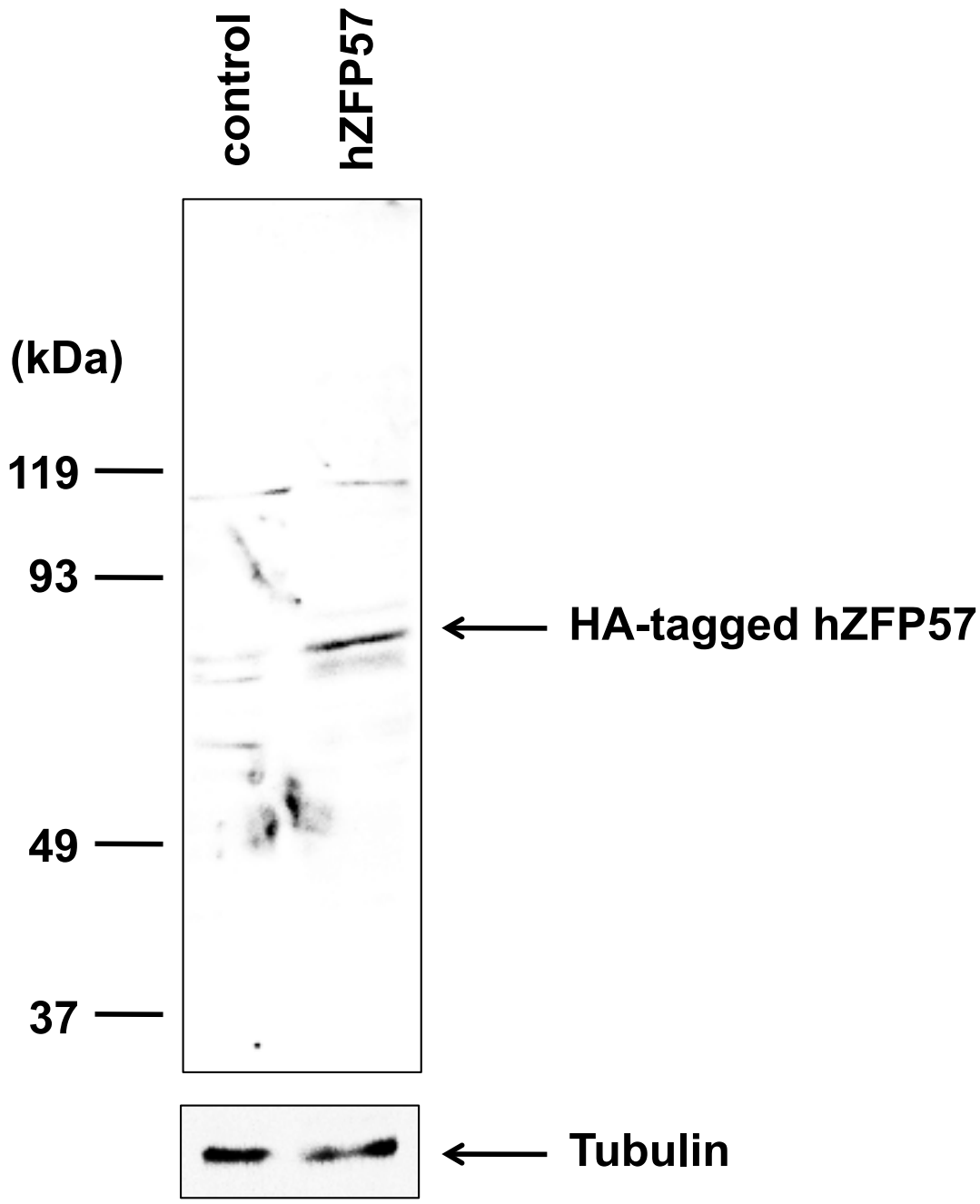

Figure S10

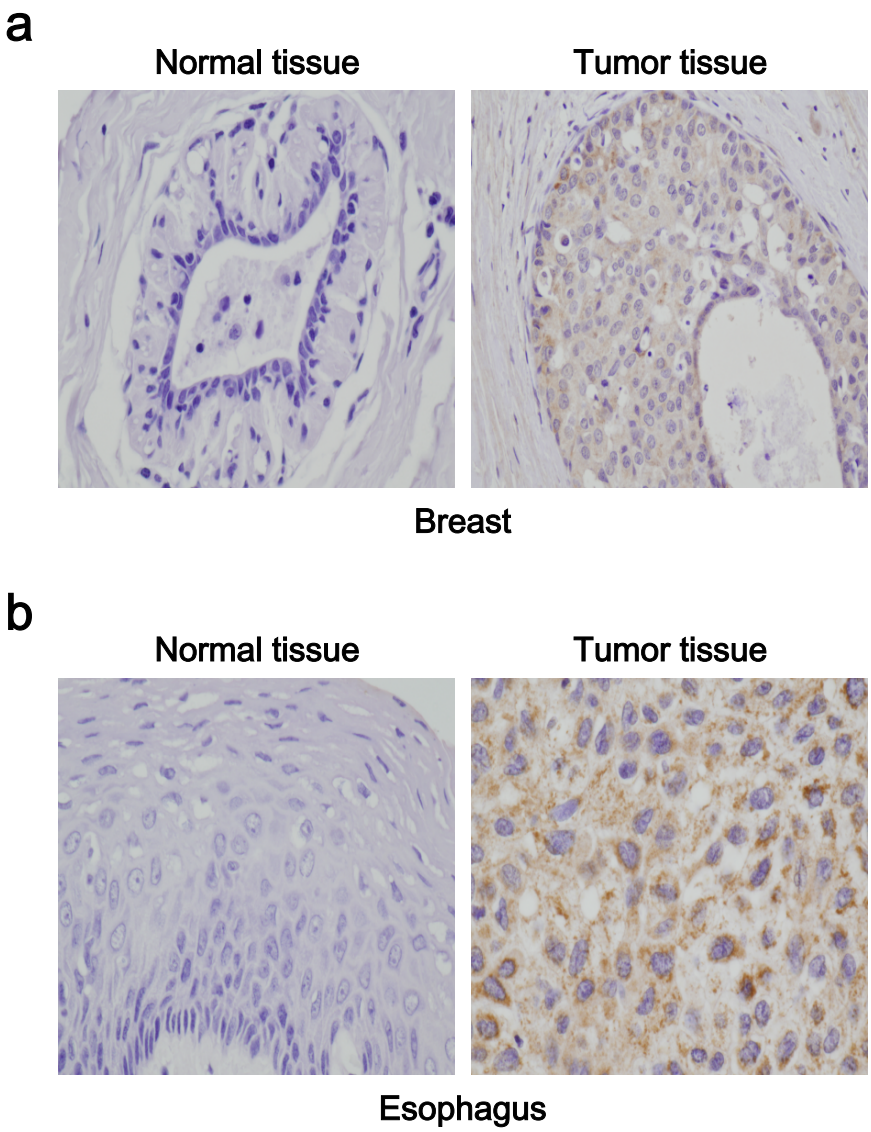
a
Normal tissue
Tumor tissue
Breast
b
Normal tissue
Tumor tissue
Esophagus